Archive of Applied Mechanics manuscript No.
(will be inserted by the editor)

E. Garrido

Few-body techniques using coordinate space for bound and continuum states

Received: date / Accepted: date

Abstract These notes are a short summary of a set of lectures given within the frame of the "Critical Stability of Quantum Few-Body Systems" International School held in the Max Planck Institute for the Physics of Complex Systems (Dresden). The main goal of the lectures has been to provide the basic ingredients for the description of few-body systems in coordinate space. The hyperspherical harmonic and the adiabatic expansion methods are introduced in detail, and subsequently used to describe bound and continuum states. The expressions for the cross sections and reaction rates for three-body processes are derived. The case of resonant scattering and the complex scaling method as a tool to obtain the resonance energy and width is also introduced.

1 Introduction

The notes presented here do not intend to cover the details of every single method developed in order to describe few-body systems in coordinate space, but mainly give the key ingredients of two of the most commonly used techniques, namely, the hyperspherical harmonic expansion and the adiabatic expansion methods. Although some relevant references containing all the details are given, we have tried to keep these notes as much self-contained as possible, in such a way that any reader non familiar with these methods can get a rather complete picture of them.

The methods themselves are described in sections 2 and 3. Although in principle they could be applied to any arbitrary A-body system, the most direct and still relatively simple application corresponds to the three-body case. In this connection, some room in section 3 has been kept to introduce the Faddeev equations and outline one of the most striking and counter-intuitive three-body phenomena, which is the Efimov effect.

The application of the methods in order to describe three-body systems in the continuum is sketched in section 4. After introducing the $\mathcal{S}$-matrix, and focusing again on three-body systems, the cross sections for the different possible three-body reactions (elastic, inelastic, breakup, recombination,...) are given in terms of the $\mathcal{S}$-matrix. Together with this, the integral relations are presented as an efficient tool leading to the extraction of the $\mathcal{S}$-matrix.

The next section, section 5, is devoted to resonant scattering. The complex scaling method is introduced as a simple procedure that permits to extract the resonance properties as poles of the $\mathcal{S}$-matrix. In the last part of the section, the general expressions derived along the text are particularized to the case of radiative processes.

Some examples of applications of the different techniques described in this work are listed in the final section 6.

This work was supported by funds provided by DGI of MINECO (Spain) under contract No. FIS2014-51971-P.

E. Garrido
Instituto de Estructura de la Materia, CSIC, Serrano 123, E-28042 Madrid, Spain
E-mail: e.garrido@csic.es

2 The Schrödinger Equation for an *A*-body system

Given an A-body system, when working in the A-body center of mass frame, the description of the $3A-3$ remaining degrees of freedom requires the introduction of $N=A-1$ vector coordinates. The natural way to do so is to construct the i^{th} coordinate as the relative coordinate between particle $i+1$ and the center of mass of i-body system, i.e.:

$$\boldsymbol{x}_i = \sqrt{\frac{\mu_i}{m}}(\boldsymbol{r}_{i+1} - \boldsymbol{R}_i) \quad (i=1,2,\cdots,N)\ ; \quad \mu_i = \frac{m_{i+1}(\sum_{j=1}^{i} m_j)}{\sum_{j=1}^{i+1} m_j} \quad \text{and} \quad \boldsymbol{R}_i = \frac{\sum_{j=1}^{i} m_j \boldsymbol{r}_j}{\sum_{j=1}^{i} m_j}, \tag{1}$$

where m_i is the mass of particle i, m is an arbitrary normalization mass, and μ_i is the reduced mass of the "two-body" system formed by the particle $i+1$ and the previous i-body system.

The inclusion of the mass factors in the definitions above allows us to write the A-body kinetic energy operator in a compact way, in terms of the normalization mass m only. In this way the A-body Schrödinger equation takes the form:

$$\left(-\frac{\hbar^2}{2m}\sum_{i=1}^{N}\boldsymbol{\nabla}_{x_i}^2 + \sum_{i<j=1}^{A} V_{ij}\right)\Psi(\boldsymbol{x}_1,\boldsymbol{x}_2,\cdots,\boldsymbol{x}_N) = E\Psi(\boldsymbol{x}_1,\boldsymbol{x}_2,\cdots,\boldsymbol{x}_N), \tag{2}$$

where V_{ij} is the interaction between particles i and j.

The $N=A-1$ generalized *Jacobi vectors* given in Eq.(1) provide the $3N=3A-3$ coordinates needed to describe a given A-body system in the center of mass frame. However, in practice, the Schrödinger Equation is usually more easily handled if these coordinates are transformed into one single radial coordinate and $3N-1=3A-4$ angular ones. This is done by means of the generalized *hyperspherical coordinates*, where the radial coordinate (*hyperradius*) and the $N-1$ *hyperangles* α_i are defined as:

$$\rho = \left[\sum_{i=1}^{N} x_i^2\right]^{1/2}, \quad \tan\alpha_i = \frac{x_i}{\sqrt{x_{i+1}^2 + x_{i+2}^2 + \cdots + x_N^2}}; \quad (i=1,2,\cdots,N-1). \tag{3}$$

The $2N$ angles $(\theta_{x_i},\varphi_{x_i})$ defining the direction of the $\boldsymbol{x}_i$ vectors constitute the remaining hyperangular coordinates. These definitions lead to the following recursive expressions for the N x_i-values: $x_i = \rho\sin\alpha_i\cos\alpha_{i-1}\cdots\cos\alpha_1$, with the understanding that $\alpha_N=\pi/2$.

It can be proved [1] that, when using the generalized hyperspherical coordinates, the kinetic energy operator in Eq.(2) takes the form:

$$-\frac{\hbar^2}{2m}\sum_{i=1}^{N}\boldsymbol{\nabla}_{x_i}^2 = -\frac{\hbar^2}{2m}\left(\frac{\partial^2}{\partial\rho^2} + \frac{3N-1}{\rho}\frac{\partial}{\partial\rho} - \frac{\hat{\Lambda}_N^2}{\rho^2}\right), \tag{4}$$

where $\hat{\Lambda}_N$ is the generalized *grand-angular momentum operator*, whose eigenfunctions are the generalized *hyperspherical harmonics* $\mathcal{Y}_{[K]}^{LM}(\Omega_N)$, where Ω_N collects the $3N-1$ hyperangles and $[K]$ contains all the quantum numbers, specified below, needed to identify a single hyperspherical harmonic. The eigenvalue corresponding to $\mathcal{Y}_{[K]}^{LM}(\Omega_N)$ is given by $K(K+3N-2)$, where $K=K_N$ with the definition:

$$K_i = K_{i-1} + \ell_{x_i} + 2n_i, \qquad (i=1,2,\cdots,N) \tag{5}$$

where n_i is a non-negative integer, ℓ_{x_i} is the relative orbital angular momentum between the particles connected by the coordinate $\boldsymbol{x}_i$, and $K_1=\ell_{x_1}$. The explicit expressions for $\hat{\Lambda}_N^2$ and $\mathcal{Y}_{[K]}^{LM}(\Omega_N)$ are found in [1; 2].

In summary, the use of the generalized hyperspherical coordinates leads to the following expression for the A-body Schrödinger Equation:

$$\left[-\frac{\hbar^2}{2m}\left(\frac{\partial^2}{\partial\rho^2} + \frac{3N-1}{\rho}\frac{\partial}{\partial\rho} - \frac{\hat{\Lambda}_N^2}{\rho^2}\right) + \sum_{i<j=1}^{A} V_{ij}\right]\Psi(\boldsymbol{x}_1,\boldsymbol{x}_2,\cdots,\boldsymbol{x}_N) = E\Psi(\boldsymbol{x}_1,\boldsymbol{x}_2,\cdots,\boldsymbol{x}_N), \tag{6}$$

where the grand-angular operator $\hat{\Lambda}_N^2$ contains the full dependence of the Hamiltonian on the $3N-1$ hyperangles ($N=A-1$).

2.1 Solving the A-body Schrödinger Equation

In order to obtain the A-body wave function $\Psi(\boldsymbol{x}_1, \boldsymbol{x}_2, \cdots, \boldsymbol{x}_N)$ it is necessary to expand it in terms of some appropriate basis set. In principle, the natural choice would be the set formed by the eigenfunctions of the $\hat{\Lambda}_N^2$ operator, i.e., the generalized hyperspherical harmonics $\{\mathcal{Y}_{[K]}^{LM}(\Omega_N)\}$. In this way, the A-body wave function is expanded as:

$$\Psi^{LM}(\boldsymbol{x}_1, \boldsymbol{x}_2, \cdots, \boldsymbol{x}_N) = \frac{1}{\rho^{(3N-1)/2}} \sum_{[K]} \chi_{[K]}^{L}(\rho) \mathcal{Y}_{[K]}^{LM}(\Omega_N), \tag{7}$$

which, when inserted into the Schrödinger Eq.(6), after multiplying from the left by $\mathcal{Y}_{[K']}^{LM*}$, integrating over the hyperangles Ω_N, and making use of the orthogonality of the hyperspherical harmonics, leads to the following set of coupled radial differential equations:

$$-\frac{\hbar^2}{2m}\left[\frac{\partial^2}{\partial\rho^2} - \frac{\mathcal{L}(\mathcal{L}+1)}{\rho^2} - E\right]\chi_{[K]}^{L}(\rho) + \sum_{[K']} \langle \mathcal{Y}_{[K]}^{LM} | \sum_{i<j=1}^{A} V_{ij} | \mathcal{Y}_{[K']}^{LM} \rangle_{\Omega_N} \chi_{[K']}^{L}(\rho) = 0, \tag{8}$$

where $\mathcal{L} = K + 3(N-1)/2$ and $\langle | \rangle_{\Omega_N}$ indicates integration over the hyperangles only.

The equations written above have been obtained assuming spinless particles. When extended to non-zero spin particles, the only difference is that the basis set used in the expansion (7) is actually formed by the generalized hyperspherical harmonics coupled to the spin function $\{\left[\mathcal{Y}_{[K]}^{L} \otimes \Sigma_{s_1\otimes\cdots\otimes s_A}^{S}\right]^{J}\}$. In order to keep the notation as clean as possible, unless the opposite is explicitly mentioned, all the expressions derived here will be obtained assuming spinless particles.

The numerical calculation of the radial wave functions $\chi_{[K]}^{L}(\rho)$ requires solving the differential equations given in Eq.(8). In order to do so the following remarks have to be taken into account:

i) The number of coupled equations is determined by the number of components included in the expansion (7). For an increasing number of particles this number can soon become exceedingly high, especially if dealing with particles with non-zero spin. Even in a simple case like the one of three identical spinless particles and a 0^+ state, one could easily have to deal with even more than $60 - 80$ coupled radial equations.

ii) The choice of the Jacobi coordinates given in Eq.(1) is not unique. There are actually $A!/2$ possible choices. If the two-body interactions V_{ij} entering in Eq.(8) are assumed to have central character, each of them will depend on a single particular relative two-body coordinate. Therefore, once the set of Jacobi coordinates has been chosen, only one of the potentials will appear in its "natural" coordinate.

iii) Due to the point above, for $A > 2$, the calculation of the potential matrix elements in Eq.(8) requires the rotation of the hyperspherical harmonics from one Jacobi set p into another set q:

$$\mathcal{Y}_{[K]}^{LM}(\Omega_p) = \sum_{[K']} R_{[K],[K']}^{pq,LM} \mathcal{Y}_{[K']}^{LM}(\Omega_q), \tag{9}$$

where the sum runs over all the quantum numbers compatible with $K = K'$, and where LM is conserved in the transformation. For three particles (3 possible Jacobi sets) the R-coefficients above are the well-known Raynal-Revai coefficients [3]. For four particles (12 possible Jacobi sets) some numerical procedures have also been developed [4].

iv) For more than four particles the number of Jacobi sets (60 for five particles or 360 for six particles) makes extremely cumbersome to implement the rotation from each Jacobi set into all the others. Nevertheless, after some appropriate cuts in the basis set, reliable numerical calculations are still possible [2].

2.2 The three-body case and the hyperspherical harmonic expansion method

All the expressions given so far can be easily particularized for the three-body case. The equations obtained constitute the well-known *hyperspherical harmonic expansion method*:

i) The coordinates given in Eq.(1) reduce to the usual *Jacobi coordinates*: $\boldsymbol{x} = \sqrt{\mu_x/m}(\boldsymbol{r}_2 - \boldsymbol{r_1})$ and $\boldsymbol{y} = \sqrt{\mu_y/m}\left(\boldsymbol{r}_3 - \frac{m_1\boldsymbol{r}_1+m_2\boldsymbol{r}_2}{m_1+m_2}\right)$, where $\mu_x = m_1m_2/(m_2+m_1)$ and $\mu_y = m_3(m_1+m_2)/(m_1+m_2+m_3)$.

ii) The the Schrödinger Equation (2) then becomes:

$$\left(-\frac{\hbar^2}{2m}(\boldsymbol{\nabla}_x^2 + \boldsymbol{\nabla}_y^2) + V_{12} + V_{13} + V_{23}\right)\Psi(\boldsymbol{x},\boldsymbol{y}) = E\Psi(\boldsymbol{x},\boldsymbol{y}). \tag{10}$$

iii) The hyperspherical coordinates (3) lead to the hyperradius $\rho = \sqrt{x^2+y^2}$ and $\alpha = \arctan(x/y)$, which together with the four angles $\Omega_x \equiv \{\theta_x, \varphi_x\}$ and $\Omega_y \equiv \{\theta_y, \varphi_y\}$ form the set of five hyperangles. The corresponding recursive relations become now $x = \rho\sin\alpha$ and $y = \rho\cos\alpha$.

iv) The kinetic energy operator in the Schrödinger equation (10) is now:

$$-\frac{\hbar^2}{2m}(\boldsymbol{\nabla}_x^2 + \boldsymbol{\nabla}_y^2) = -\frac{\hbar^2}{2m}\left(\frac{\partial^2}{\partial\rho^2} + \frac{5}{\rho}\frac{\partial}{\partial\rho} - \frac{\hat{\Lambda}^2}{\rho^2}\right), \tag{11}$$

where the grand-angular operator $\hat{\Lambda}^2$ takes the form:

$$\hat{\Lambda}^2 = -\frac{\partial^2}{\partial\alpha^2} - 4\cot(2\alpha)\frac{\partial}{\partial\alpha} + \frac{\hat{L}_x^2}{\sin^2\alpha} + \frac{\hat{L}_y^2}{\cos^2\alpha}, \tag{12}$$

whose eigenfunctions, which are the particularization of the angular functions $\mathcal{Y}^{LM}_{[K]}(\Omega_N)$ to three particles, are the hyperspherical harmonics:

$$\mathcal{Y}^{LM}_{K\ell_x\ell_y}(\Omega) = N_K^{\ell_x\ell_y}(\sin\alpha)^{\ell_x}(\cos\alpha)^{\ell_y}P_n^{(\ell_x+\frac{1}{2},\ell_y+\frac{1}{2})}(\cos 2\alpha)\left[Y_{\ell_x}(\Omega_x)\otimes Y_{\ell_y}(\Omega_y)\right]^{LM}. \tag{13}$$

In the expression above Ω collects the five hyperangles, $N_K^{\ell_x\ell_y}$ is a normalization factor, $P_n^{(\ell_x+\frac{1}{2},\ell_y+\frac{1}{2})}$ is a Jacobi polynomial, L is the coupling of ℓ_x and ℓ_y, and K ($K = 2n+\ell_x+\ell_y$ with $n = 0, 1, \cdots$) is the hypermomentum. The eigenvalue corresponding to the eigenfunction $\mathcal{Y}^L_{K\ell_x\ell_y}(\Omega)$ is $K(K+4)$.

v) Therefore, the three-body Schrödinger equation is finally written as:

$$\left[-\frac{\hbar^2}{2m}\left(\frac{\partial^2}{\partial\rho^2} + \frac{5}{\rho}\frac{\partial}{\partial\rho} - \frac{\hat{\Lambda}^2}{\rho^2}\right) + V_{12} + V_{13} + V_{23})\right]\Psi(\boldsymbol{x},\boldsymbol{y}) = E\Psi(\boldsymbol{x},\boldsymbol{y}), \tag{14}$$

which, following Eq.(7) and below, is solved by means of the expansion:

$$\Psi^{LM}(\boldsymbol{x},\boldsymbol{y}) = \frac{1}{\rho^{5/2}}\sum_{K\ell_x\ell_y}\chi^L_{K\ell_x\ell_y}(\rho)\mathcal{Y}^{LM}_{K\ell_x\ell_y}(\Omega), \tag{15}$$

and leads to the coupled set of radial differentials equations:

$$\left[-\frac{\hbar^2}{2m}\left(\frac{\partial^2}{\partial\rho^2} - \frac{(K+\frac{3}{2})(K+\frac{5}{2})}{\rho^2}\right) - E\right]\chi^L_{K\ell_x\ell_y}(\rho) + \sum_{K'\ell'_x\ell'_y}\langle\mathcal{Y}^{LM}_{K\ell_x\ell_y}|\sum_{i<j=1}^{3}V_{ij}|\mathcal{Y}^{LM}_{K'\ell'_x\ell'_y}\rangle_\Omega\chi^L_{K'\ell'_x\ell'_y}(\rho) = 0. \tag{16}$$

vi) Once the Jacobi set has been chosen the potential matrix elements in Eq.(16) involve terms like $\langle\mathcal{Y}^{LM}_{K\ell_{x_i}\ell_{y_i}}(\Omega_i)|V_{ik}(x_j)|\mathcal{Y}^{LM}_{K'\ell'_{x_i}\ell'_{y_i}}(\Omega_i)\rangle_{\Omega_i}$, where i and j refer to two different sets of Jacobi coordinates. The calculation of the such a matrix element requires rotation of the hyperspherical harmonics from the Jacobi set i into the Jacobi set j. This is done by means of:

$$\mathcal{Y}^{LM}_{K\ell_{x_i}\ell_{y_i}}(\Omega_i) = \sum_{\ell_{x_j}\ell_{y_j}}\langle\mathcal{Y}^{LM}_{K\ell_{x_j}\ell_{y_j}}(\Omega_j)|\mathcal{Y}^{LM}_{K\ell_{x_i}\ell_{y_i}}(\Omega_i)\rangle\mathcal{Y}^{LM}_{K\ell_{x_j}\ell_{y_j}}(\Omega_j), \tag{17}$$

where the transformation preserves the values of K, L, and M, and where the set of coefficients $\langle\mathcal{Y}^{LM}_{K\ell_{x_j}\ell_{y_j}}(\Omega_j)|\mathcal{Y}^{LM}_{K\ell_{x_i}\ell_{y_i}}(\Omega_i)\rangle$ are the so-called Raynal-Revai coefficients [3].

3 The three-body problem and the adiabatic expansion method

As already discussed, the number of coupled equations in (16) is determined by the size of the basis set used in the expansion of the three-body wave function (15). Although the relative orbital angular momenta ℓ_x and ℓ_y are usually limited to rather modest values, this is not true anymore for the quantum number K, and the number of radial wave functions to be evaluated can be significantly high. This number can be drastically reduced by use of the *adiabatic expansion method*, whose starting point is replacing the expansion of the three-body wave function by the more general form:

$$\Psi^{LM}(\boldsymbol{x},\boldsymbol{y}) = \frac{1}{\rho^{5/2}} \sum_n f_n^L(\rho) \Phi_n^{LM}(\rho,\Omega), \tag{18}$$

where $\{\Phi_n^{LM}(\rho,\Omega)\}$ constitutes a complete basis set whose explicit form will be given later on. Note that the basis terms depend not only on the hyperangles, but also on the hyperradius. Note as well that here n is not a quantum number, but just a label numbering the different angular functions.

If we insert the expansion (18) into the Schrödinger Equation (14) we obtain:

$$\sum_{n'} \left[-\frac{\partial^2 f_{n'}}{\partial\rho^2}\Phi_{n'} + \frac{15}{4}\frac{1}{\rho^2} f_{n'}\Phi_{n'} - 2\frac{\partial f_{n'}}{\partial\rho}\frac{\partial\Phi_{n'}}{\partial\rho} - f_{n'}\frac{\partial^2\Phi_{n'}}{\partial\rho^2} - \frac{2mE}{\hbar^2} f_{n'}\Phi_{n'} \right] + \\ + \sum_{n'} \frac{f_{n'}}{\rho^2} \left[\hat{\Lambda}^2\Phi_{n'} + \frac{2m\rho^2}{\hbar^2}(V_{12}+V_{13}+V_{23})\Phi_{n'} \right] = 0, \tag{19}$$

where for simplicity in the notation the L and M indexes have been omitted.

The key point of the method is that in the expression above all the operators depending on the hyperangles are contained within the last bracket. This is exploited in order to choose the angular functions $\Phi_n(\rho,\Omega)$ as the eigenfunctions of this angular part of the Schrödinger equation. Namely,

$$\left[\hat{\Lambda}^2 + \frac{2m\rho^2}{\hbar^2}(V_{12}+V_{13}+V_{23}) \right] \Phi_n(\rho,\Omega) = \lambda_n(\rho)\Phi_n(\rho,\Omega). \tag{20}$$

This means that the basis set used in the expansion in Eq.(18) is the one formed by the eigenfunctions of the angular part of the Schrödinger equation. Therefore, they satisfy that $\int d\Omega \Phi_n^*(\rho,\Omega)\Phi_{n'}(\rho,\Omega) = \delta_{nn'}$ for any value of the hyperradius ρ. In fact, Eq.(20) is solved for each value of ρ, which is treated as a parameter. This gives rise to a set of eigenvalues $\lambda_n(\rho)$, which are functions of the hyperradius.

If we now multiply Eq.(19) from the left by $\Phi_n^*(\rho,\Omega)$ and make use of Eqs.(20) and the orthogonality of the eigenfunctions, we then easily get that the radial wave functions $f_n(\rho)$ appear as the solution of the following coupled set of equations:

$$\left[-\frac{\partial^2}{\partial\rho^2} + \frac{\lambda_n(\rho)+\frac{15}{4}}{\rho^2} - \frac{2mE}{\hbar^2} \right] f_n(\rho) - \sum_{n'} \left(2P_{nn'}(\rho)\frac{\partial}{\partial\rho} + Q_{nn'}(\rho) \right) f_{n'}(\rho) = 0, \tag{21}$$

where the coupling functions $P_{nn'}(\rho)$ and $Q_{nn'}(\rho)$ are given by:

$$P_{nn'}(\rho) = \langle \Phi_n(\rho,\Omega) | \frac{\partial}{\partial\rho} | \Phi_{n'}(\rho,\Omega) \rangle_\Omega, \quad Q_{nn'}(\rho) = \langle \Phi_n(\rho,\Omega) | \frac{\partial^2}{\partial\rho^2} | \Phi_{n'}(\rho,\Omega) \rangle_\Omega. \tag{22}$$

Therefore, in the adiabatic expansion method the three-body problem (14) is solved in two steps. First, the angular equation (20) is solved for different values of ρ. The angular eigenfunctions are then used as a basis set to expand the three-body wave function. Finally, in the second step, the radial wave functions $f_n(\rho)$ are obtained by solving the coupled set of differential equations (21), where the eigenvalues λ_n of the angular part enter as effective potentials, and where the corresponding eigenfunctions Φ_n determine the coupling terms given in Eq.(22).

3.1 Some properties of the angular eigenvalues and eigenfunctions

From the angular equation (20) it is obvious that for $\rho = 0$, and provided the two-body potentials do not diverge at the origin faster than $1/\rho^2$, the angular equation is just $\hat{\Lambda}^2\Phi_n = \lambda_n\Phi_n$. This implies that at the origin the angular eigenfunctions are just the hyperspherical harmonics and $\lambda_n(\rho = 0) = K(K+4)$. In the same way, when dealing with short-range potentials, i.e., when the two-body potentials go to zero at large distances faster than $1/\rho^2$, the same discussion applies, and $\lambda_n(\rho = \infty) = K(K + 4)$.

The large distance behavior given above is valid only when none of the internal two-body subsystems has a bound state (i.e., when the three-body system has borromean character). If this is not the case, and we assume that the potential $V_{12}(x)$ is able to bind particles 1 and 2, we then have that for $\rho \to \infty$ $V_{12}(x)$ survives, and the angular equation (20) can be written for large values of ρ as

$$\left[-\frac{\partial^2}{\partial\alpha^2} - 4\cot(2\alpha)\frac{\partial}{\partial\alpha} + \frac{\ell_x(\ell_x+1)}{\sin^2\alpha} + \frac{\ell_y(\ell_y+1)}{\cos^2\alpha} + \frac{2m\rho^2}{\hbar^2}V_{12}(x)\right]\phi_n^{\ell_x\ell_y}(\rho,\alpha) = \lambda_n(\rho)\phi_n^{\ell_x\ell_y}(\rho,\alpha), \tag{23}$$

where Eq.(12) has been used, and where the angular functions Φ_n have been decomposed into partial waves, i.e., $\Phi_n(\rho,\Omega) = \sum_{\ell_x\ell_y}\phi_n^{\ell_x\ell_y}(\rho,\alpha)\left[Y_{\ell_x}(\Omega_x)\otimes Y_{\ell_y}(\Omega_y)\right]^{LM}$.

This picture, even though $\rho \to \infty$, corresponds to $x \ll y$. Therefore, keeping up to the terms linear in α ($\sin\alpha \sim \alpha$, $\cos\alpha \sim 1$, and $x \sim \rho\alpha$), we can easily see that for $\rho \to \infty$ the dominating term in Eq.(23) is given by:

$$\frac{2m\rho^2}{\hbar^2}\left[-\frac{\hbar^2}{2\mu_{12}}\left(\frac{\partial^2}{\partial r_{12}^2} + \frac{2}{r_{12}}\frac{\partial}{\partial r_{12}} - \frac{\ell_x(\ell_x+1)}{r_{12}^2}\right) + V(r_{12})\right]\phi_n^{\ell_x\ell_y}(r_{12}) = \lambda_n(\rho)\phi_n^{\ell_x\ell_y}(r_{12}), \tag{24}$$

where r_{12} is the relative distance between the two particles in the dimer and μ_{12} is the reduced mass.

In Eq.(24) the expression within the squared brackets is nothing but the radial two-body Schrödinger equation. Therefore, if the two-body bound state has a binding energy $E_{2b}^{(n)}$ (< 0), we then have:

$$\lambda_n(\rho) \overset{\rho\to\infty}{\longrightarrow} -\frac{2m|E_{2b}^{(n)}|}{\hbar^2}\rho^2, \tag{25}$$

in such a way that if we define the effective adiabatic potentials entering in the equations (21) as

$$V_n^{eff}(\rho) = \frac{\hbar^2}{2m}\frac{\lambda_n(\rho) + \frac{15}{4}}{\rho^2}, \tag{26}$$

we trivially have that for those adiabatic channels associated to a bound two-body dimer the effective potential satisfies $V_n^{eff}(\rho) \overset{\rho\to\infty}{\to} -|E_{2b}^{(n)}|$.

The discussion in this subsection proves one of the most important properties of the adiabatic expansion method. Namely, in the expansion given in Eq.(18), the channels corresponding to an asymptotic bound dimer+particle structure are separated from those where none of the two-body subsystems is bound. Whereas the first ones are easily identified by the asymptotic behaviour (26), the second ones follow the hyperspherical $K(K + 4)$ spectrum.

As an illustration we show in Fig.1 the lowest λ-functions for ^{11}Li (left) and hypertriton (right). Due to its borromean character, for ^{11}Li all the λ-functions reproduce the hyperspherical spectrum $K(K+4)$ are large distances. For hypertriton, where the neutron and the proton can bind into deuteron, the lowest λ-function behaves asymptotically as dictated by Eq.(25).

3.2 The Faddeev equations

We have already mentioned the fact that the Jacobi coordinates (1) are not unique. In fact, there are $A!/2$ possible sets. Of course, given a particular system, it is important to choose the most appropriate set. Let us for instance consider a three-body system where one of the two-body subsystems presents a bound state. It seems then natural to choose the Jacobi coordinates such that the $\boldsymbol{x}$-coordinate connects the two particles holding the bound state. In this way, the strong correlation between these two particles, present even for large values of the hyperradius, is more accurately described. A different

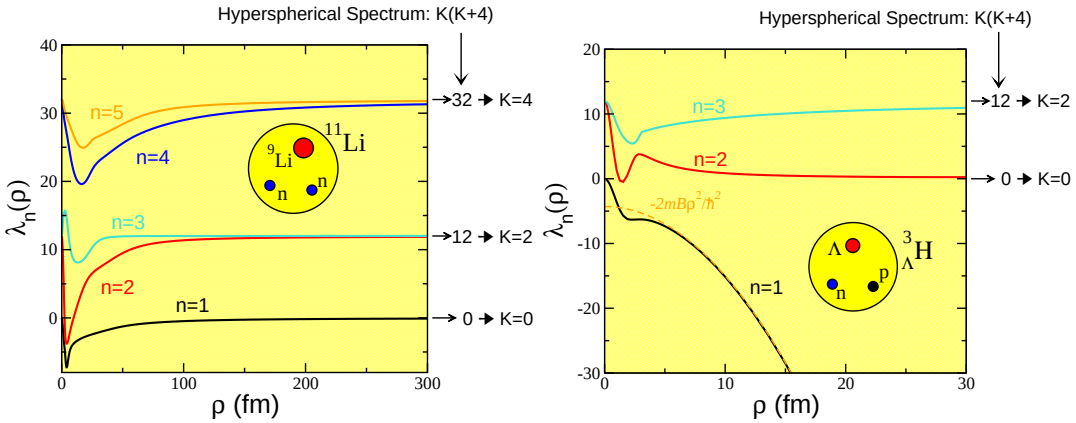

Fig. 1 Lowest λ-functions for ^{11}Li (left), where the short-range two-body potentials do not hold any bound state, and for hypertriton (right), where the neutron-proton interaction can bind the system into deuteron. The orange-dashed curve corresponds to Eq.(25) with $B = E_{2b}^{(1)} = -2.22$ MeV.

choice would require a much larger expansion of the three-body wave function in order to correctly reproduce the asymptotic behaviour of the adiabatic effective potential given by Eq.(25).

However, the choice is not so clear when two of the two-body subsystems are strongly correlated, as for instance when two bound two-body subsystems are present. In this case it is inevitable to describe one of these subsystems using a non-natural coordinate, and, therefore, the geometry corresponding to this bound state plus the third particle far away is very likely poorly described. One way to alleviate this deficiency is to introduce the *Faddeev equations*, where all the possible Jacobi sets are equally treated.

The starting point here is to write the full wave function as a sum of components, each of them written in terms of one of the possible Jacobi sets, i.e., $\Psi = \sum_{i=1}^{A!/2} \psi_i(\boldsymbol{x}_1^i, \boldsymbol{x}_2^i, \cdots, \boldsymbol{x}_N^i)$, and then solve the set of $A!/2$ equations $T\psi_i + V_i\Psi = E\psi_i$ with $i = 1, \cdots, A!/2$, and where V_i denotes the interaction between the particles connected by the Jacobi coordinate $\boldsymbol{x}_1^i$. Note that the sum of the $A!/2$ equations is nothing but the Schrödinger equation.

Being more specific, for a three-body system and the adiabatic expansion given in Eq.(18), we write the angular eigenfunctions Φ_n as the sum of three components, each of them written in terms of one of the three possible Jacobi sets:

$$\Phi_n(\rho, \Omega) = \phi_n^{(1)}(\rho, \Omega_1) + \phi_n^{(2)}(\rho, \Omega_2) + \phi_n^{(3)}(\rho, \Omega_3), \tag{27}$$

in such a way that each of the components satisfies the angular Faddeev equations:

$$\left(\hat{\Lambda}^2 - \lambda_n(\rho)\right)\phi_n^{(i)} + \frac{2m\rho^2}{\hbar^2} V_i(x_i)(\phi_n^{(1)} + \phi_n^{(2)} + \phi_n^{(3)}) = 0 \tag{28}$$

where $V_i \equiv V_{jk}$ is the interaction between particles j and k and where the summation of the three equations gives the original angular Schrödinger equation (20).

In actual calculations the Faddeev components $\phi_n^{(i)}$ are expanded in terms of the hyperspherical harmonics, $\phi_n^{(i)}(\rho, \Omega_i) = \sum_{K\ell_x\ell_y} C_{K\ell_x\ell_y}^{n(i)}(\rho)\mathcal{Y}_{K\ell_x\ell_y}^{LM}(\Omega_i)$, which transforms the angular Faddeev equations (28) into an eigenvalue problem for each ρ where the calculation of the necessary matrix elements $\langle \mathcal{Y}_{K\ell_x\ell_y}^{LM}(\Omega_i)|V_i|\phi_1^{(1)} + \phi_1^{(2)} + \phi_1^{(3)}\rangle$ requires rotation of the components $\phi_n^{(j)}$ and $\phi_n^{(k)}$ into the Jacobi set i. This is done by means of Eq.(17). For large values of K this transformation can involve a large number of terms, and very often it is convenient to truncate it, which can be a source of inaccuracies. In any case, the solution of the Faddeev equations is linear in this transformation, whereas the calculation of the matrix elements in (16) is quadratic in the same transformation. The details of the method described above, the so-called *hyperspherical adiabatic expansion method*, are given in [5].

3.3 The Efimov effect

We have learned that the asymptotic behaviour of the angular eigenvalues λ_n can either diverge according to Eq.(25), which is associated to the existence of a bound dimer with energy E_{2b}, or go to the $K(K+4)$ hyperspherical spectrum (assuming short-range potentials). In the first case, it is clear that the closer E_{2b} to zero the smaller the curvature of the diverging parabola. In fact, one could intuitively think that, eventually, for $E_{2b}=0$, the corresponding λ-function should go to some constant value. This is actually what happens [5; 6; 7], and we shall denote this constant value (which is in fact the next term in the expansion that led to Eq.(25)) as λ_∞.

It is important to remember that for weakly bound two-body systems and relative s-waves the two-body binding energy can be obtained as $E_{2b}=-\hbar^2/(2\mu a^2)$, where μ is the two-body reduced mass and a is the scattering length of the two-body potential. Therefore, when dealing with weakly bound two-body subsystems we are actually dealing with large scattering lengths, which is in fact infinity (*unitary limit*) when $E_{2b}=0$.

Let us consider now a three-body system such that the two-body potentials produce one zero-energy two-body state. In this case, for large ρ's, where the radial equations (21) decouple, we have that the equation corresponding to the zero energy adiabatic channel reads:

$$\left[-\frac{\partial^2}{\partial\rho^2}+\frac{\lambda_\infty+\frac{15}{4}}{\rho^2}-\frac{2mE}{\hbar^2}\right]f(\rho)=0, \tag{29}$$

which, for bound states ($E<0$), can be conveniently rewritten as:

$$\left[-\frac{\partial^2}{\partial\rho^2}+\frac{\nu_\infty^2-\frac{1}{4}}{\rho^2}+\kappa_n^2\right]f(\rho)=0, \tag{30}$$

where $\nu_\infty^2=\lambda_\infty+4$, and $\kappa_n^2=2m|E_n|/\hbar^2$. The index n labels all the possible bound states.

The equation above is actually valid not only when $|a|=\infty$, but in the region where $\rho_0\ll\rho\ll|a|$, where ρ_0 is the range of the interaction. It is in this region where the λ-function takes a constant value, which we shall still denote as λ_∞.

The good thing about Eq.(30) is that its solution is analytical, and, as seen by making use of 9.6.1 of [8], it is given by $f(\rho)\propto\sqrt{\kappa_n\rho}K_{\nu_\infty}(\kappa_n\rho)$, where K_{ν_∞} is a modified Bessel function of second kind. This function decays exponentially at large distances ($f(\rho)\overset{\kappa_n\rho\to\infty}{\longrightarrow}e^{-\kappa_n\rho}$), as expected for bound states.

In the other extreme, $\kappa_n\rho\to0$ (which means very small three-body energies), the solution of Eq.(30) behaves as

$$f(\rho)\overset{\kappa_n\rho\to0}{\longrightarrow}\sqrt{\kappa_n\rho}\left((\kappa_n\rho)^{\nu_\infty}-(\kappa_n\rho)^{-\nu_\infty}\right), \tag{31}$$

which implies that, in general, for $\nu_\infty^2=|\nu_\infty|^2>0$, the low-energy solution diverges.

However, things are very different when $\nu_\infty^2=-|\nu_\infty|^2<0$ (or $\lambda_\infty<-4$). In this case ν_∞ is pure imaginary ($\nu_\infty=i|\nu_\infty|$), and the low-energy behaviour (31) becomes:

$$f(\rho)\overset{\kappa_n\rho\to0}{\longrightarrow}\sqrt{\kappa_n\rho}\sin(|\nu_\infty|\ln(\kappa_n\rho)), \tag{32}$$

which is valid within the hyperradius range $\rho_0\ll\rho\ll|a|$, where Eq.(30) is also valid, and it is an oscillating function whose zeros appear periodically for $|\nu_\infty|\ln(\kappa_n\rho)=n\pi$.

It is well known that the number of zeros of a wave function indicates the number of excited states of the system. In this way, if for a given ρ the wave function has a zero for some value of κ_n, we know that all the following excited states, with momenta $\kappa_{n+1},\kappa_{n+2},\cdots$, have a zero at the same ρ-value. In other words, given the state with momentum κ_n and a zero at a given ρ, the next excited state will appear at the momentum κ_{n+1} and it will have a zero at the same ρ. We therefore have that $|\nu_\infty|\ln(\kappa_n\rho)-|\nu_\infty|\ln(\kappa_{n+1}\rho)=\pi$, which means that $\kappa_{n+1}=\kappa_n e^{-\pi/|\nu_\infty|}$. Taking now into account that $\kappa_n^2=2m|E_n|/\hbar^2$, we then get that for small energies the excited states scale according to

$$E_n=E_0e^{-\frac{2\pi}{|\nu_\infty|}n}, \tag{33}$$

where E_0 is the energy of the ground state. Furthermore, it simple to see that $E_n/E_0 = \langle\rho^2\rangle_0/\langle\rho^2\rangle_n$, which leads to $\langle\rho^2\rangle_n = \langle\rho^2\rangle_0 e^{\frac{2\pi}{|\nu_\infty|}n}$, which implies that, given two consecutive states, the decreasing factor between their energies is the same as the increasing factor for the corresponding $\langle\rho^2\rangle$-values.

In the limit of very small binding energies (and $\nu_\infty^2 = -|\nu_\infty|^2$), Eq.(30) can be approximated by

$$\left[-\frac{\partial^2}{\partial\rho^2} - \frac{|\nu_\infty|^2 + \frac{1}{4}}{\rho^2}\right] f(\rho) = 0, \tag{34}$$

which can be solved after regularization of the $(|\nu_\infty|^2 + 1/4)/\rho^2$ function, which is made constant and equal to $(|\nu_\infty|^2 + 1/4)/\rho_0^2$ for $\rho < \rho_0$. As one can easily check, the solution of Eq.(34) takes the form, $f(\rho) \propto \sqrt{\rho}\sin\left(|\nu_\infty|\ln(\rho/\rho_0) + \delta\right)$, where δ is a phase depending on the boundary condition at $\rho = \rho_0$. This expression, is an accurate approximation of Eq.(32) for very small energies, and gives the long distance behaviour of the radial wave function in the region $\rho_0 \ll \rho \ll |a|$. Within this region, up to $\rho = |a|$, the number of zeros N of the wave function can be obtained by making the argument of the sinus function equal to $N\pi$, from which we obtain $N \approx \frac{|\nu_\infty|}{\pi}\ln\left(\frac{|a|}{\rho_0}\right)$.

It is now obvious that in the unitary limit ($|a| = \infty$) the system has infinitely many zeros, or, in other words, infinitely many excited states. The same happens for zero-range interactions ($\rho_0 = 0$) which is known as the Thomas collapse. In summary, in the unitary limit, and provided that $\lambda_\infty < -4$, i.e. $\nu_\infty^2 < 0$, the system has infinitely many excited states whose excitation energies scale according to Eqs.(33). These are the so-called *Efimov states*.

3.3.1 Additional remarks

A detailed analysis of the large distance behavior of the λ-functions can be found in [5; 7]. From this analysis the following important results are obtained:

1.- When the bound two-body states appear for relative orbital angular momenta larger than zero the λ-functions reproduce asymptotically the free spectrum ($\lambda \to K(K+4)$) no matter the binding energies and the properties of the two-body potentials. Therefore, even if the two-body energies are small, the condition $\lambda_\infty < -4$ is not fulfilled and the Efimov states are not present.

2.- If we then focus on s-wave bound two-body states, the general result is that for large values of ρ the behaviour of the λ-functions is determined by making equal to zero the determinant of a 3×3 matrix M whose terms are given by [9; 10]:

$$M_{ii} = \nu\cos\left(\nu(\rho)\frac{\pi}{2}\right) - \sin\left(\nu(\rho)\frac{\pi}{2}\right)\frac{\rho}{\sqrt{\mu_i/m}}\frac{1}{a_i}\ ;\ \ M_{i\neq j} = \frac{2\sin\left[\nu(\rho)(\gamma_{ij} - \frac{\pi}{2})\right]}{\sin(2\gamma_{ij})}, \tag{35}$$

and

$$\gamma_{ij} = \arctan\left[\frac{m_k(m_1+m_2+m_3)}{m_i m_j}\right]^{1/2}, \tag{36}$$

where $\nu^2(\rho) = \lambda(\rho) + 4$.

3.- If the three two-body scattering lengths a_i remain finite ($|a_i| \ll \rho$ for $i = 1, 2, 3$) the expressions above lead to the already known result that, asymptotically, the λ-functions reproduce the $K(K+4)$ spectrum. Also, if only one of the scattering lengths is very large, ($|a_1|, |a_2| \ll \rho \ll |a_3|$) then λ_∞ never fulfills the condition $\lambda_\infty < -4$. Therefore, when at most one of the two-body subsystems presents a bound state at zero energy the Efimov states are not present either.

4.- When dealing with s-wave two-body states, and when at least two of the two-body scattering lengths are large, i.e. $|a_1| \ll \rho \ll |a_2|, |a_3|$ or $\rho \ll |a_1|, |a_2|, |a_3|$, the condition $\lambda_\infty < -4$ ($\nu_\infty^2 < 0$) is always satisfied, and the Efimov states show up.

5.- As easily seen from Eqs.(35) and (36), the value of $|\nu_\infty|$, which determines the scaling factor between the energies of two consecutive Efimov states, strongly depends on the mass of the particles. For three identical bosons we obtain $\nu_\infty = -1.00624$, which leads to $\lambda_\infty = -5.01251$. This value implies a factor of ~ 515 for two consecutive energies. For a system with identical particles 1 and 2, a very small scattering length for the interaction between them, and a large scattering length for the interaction between particles 1 and 2 with particle 3, one finds that the most unfavored situation corresponds to the case where particle 3 is much heavier than 1 and 2 (if $m_3 \approx 20 m_1$ then $|\nu_\infty| = 0.0453$, and scale factor is $\sim 10^{60}$). On the contrary, the most favorable situation appears when 1 and 2 are much heavier than 3 (if $m_3 \approx m_1/20$ then $|\nu_\infty| = 1.8984$, and the scale factor is 27.6). See Fig.2 for an illustration.

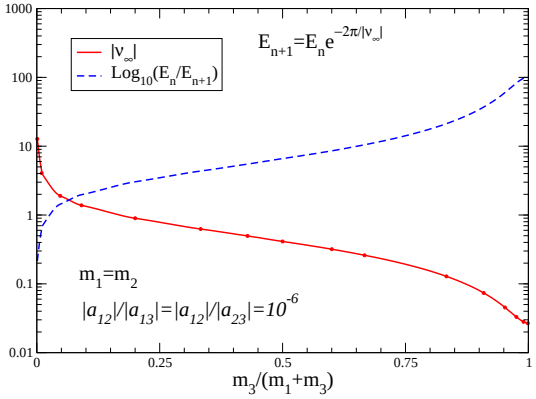

Fig. 2 Computed values of $|\nu_\infty|$ (red-solid curve) and the logarithm of the corresponding scale factor between consecutive energies (blue-dashed curve) for a three-body system containing two identical particles as function of $m_3/(m_1+m_3)$, where the index 3 corresponds to the non-identical particle. The scattering length $|a_{12}|$ for the interaction between particles 1 and 2 is six orders of magnitude smaller than the one corresponding to the interactions between particles 1 and 3 and between particles 2 and 3.

4 Continuum states and the $\mathcal{S}$-matrix

Solving the Schrödinger equation (16) or (21) in the continuum (positive values of the energy) leads to solutions whose asymptotic behaviour is dictated by the differential equation:

$$\left[-\frac{\partial^2}{\partial\rho^2}-\frac{2mE}{\hbar^2}\right]f(\rho)=0, \tag{37}$$

whose general form is just a linear combination of sinus and cosinus functions. This fact immediately implies that continuum wave functions are not square integrable. Continuum systems are therefore not localized in the space, and, after interacting, the particles involved in the system move far apart from each other. Therefore, in general, the description of an N-body system in the continuum requires knowledge of three different ingredients: *i)* How the N particles get close to each other, *ii)* how they interact, and *iii)* how they move far apart from each other. In other words, the description of a system in the continuum is equivalent to describing the collision between the particles involved in the system under investigation.

Let us start by considering Ψ_{ini} as the wave function of the full system in some initial state (often denoted as $\Psi(t=-\infty)$). We then let the particles collide and denote as Ψ_{fin} the wave function of the system at $t=\infty$ after the collision, i.e., $\Psi_{fin}\equiv\Psi(t=\infty)$. If we now admit that there exist an operator $\hat{\mathcal{S}}$ such that $\Psi_{fin}=\hat{\mathcal{S}}\Psi_{ini}$, then, due to the probability conservation ($\langle\Psi_{ini}|\Psi_{ini}\rangle=\langle\Psi_{fin}|\Psi_{fin}\rangle$) we immediately get that $\hat{\mathcal{S}}^\dagger\hat{\mathcal{S}}=\mathbb{1}$. In other words, $\hat{\mathcal{S}}$ is a unitary operator.

In this way, we can also write

$$\Psi_{fin}=\Psi_{ini}+(\hat{\mathcal{S}}-1)\Psi_{ini}=\Psi_{ini}+\hat{\mathcal{T}}\Psi_{ini}, \tag{38}$$

where $\hat{\mathcal{T}}=\hat{\mathcal{S}}-\mathbb{1}$ is the transition operator, and $\hat{\mathcal{T}}\Psi_{ini}$ contains the information about all possible scattering processes. Obviously, in case of no interaction between the particles we have $\hat{\mathcal{S}}=\mathbb{1}$ and $\hat{\mathcal{T}}=0$.

Let us assume now that Ψ_{ini} and Ψ_{fin} are expanded in terms of some orthogonal basis set $\{|\varphi_\alpha\rangle\}$. Thus, $\Psi_{fin}=\sum_\alpha c^f_\alpha|\varphi_\alpha\rangle=\sum_\alpha c^i_\alpha\hat{\mathcal{S}}|\varphi_\alpha\rangle$, and using the orthogonality of the basis terms we get:

$$c^f_\beta=\langle\varphi_\beta|\Psi_f\rangle=\sum_\alpha c^i_\alpha\langle\varphi_\beta|\hat{\mathcal{S}}|\varphi_\alpha\rangle=\sum_\alpha\mathcal{S}_{\beta\alpha}c^i_\alpha, \tag{39}$$

where the matrix formed by all the possible $\mathcal{S}_{\alpha\beta}$-terms is the so-called $\mathcal{S}$-*matrix*.

If initially the system is in a state α_0 we then have that $c^i_\alpha=\delta_{\alpha\alpha_0}$, which means that $c^f_\beta=\mathcal{S}_{\beta\alpha_0}$. Therefore, $|\mathcal{S}_{\beta\alpha}|^2$ gives the probability of finding the system after the collision in a state β, if initially the

system was in the state α. All the possible initial and final states are usually called *channels* (entrance or incoming channels, and outgoing or exit channels). Those channels accessible to the system are called *open* channels, whereas those ones that for whatever reason can not be populated are called *closed* channels. Obviously the dimension of the $\mathcal{S}$-matrix is given by the number of open channels in the collision under study. Also, making use of the unitarity condition we have that $\sum_\beta |\mathcal{S}_{\beta\alpha}|^2 = 1$, which simply means that after the collision the system has to be in one of the available final states.

Together with the $\mathcal{S}$-matrix it is common to use the $\mathcal{K}$-matrix instead to describe the reaction. The connection between both matrices is $\mathcal{S} = (1 + i\mathcal{K})(1 - i\mathcal{K})^{-1}$, which implies that $\mathcal{K} = \mathcal{K}^\dagger$. Therefore, the eigenvalues of $\mathcal{K}$ are real, which often makes possible to work with real quantities only.

4.1 The two-body case with central potentials

Let us first consider the simple case of a two-body system made of two inert particles characterized by some initial state $|i\rangle \equiv |\ell_i m_i\rangle$. If the two-body interaction can in principle mix different ℓ and m values, we then have that after the collision the system can be found in some state $|f\rangle \equiv |\ell m\rangle$, which could be different from the initial one.

In case of no interaction between the particles, the continuum wave function (solution of Eq.(37)) reduces to the plane wave $e^{i\boldsymbol{k}\cdot\boldsymbol{r}}$, where $\boldsymbol{k}$ is the relative two-body momentum. As it is well-known, the plane wave can be expanded in partial waves as:

$$e^{i\boldsymbol{k}\cdot\boldsymbol{r}} = 4\pi \sum_{\ell m} i^\ell j_\ell(kr) Y_{\ell m}(\theta_r, \varphi_r) Y^*_{\ell m}(\theta_k, \varphi_k), \tag{40}$$

where $j_\ell(kr)$ the is regular spherical Bessel function.

This expansion immediately suggests the following form for the general continuum two-body wave function:

$$\Psi_{\boldsymbol{k}}(\boldsymbol{r}) = 4\pi \sum_{i,f} i^\ell \frac{u_{fi}(r)}{kr} Y_{\ell m}(\theta_r, \varphi_r) Y^*_{\ell_i m_i}(\theta_k, \varphi_k), \tag{41}$$

where the radial function u_{fi} is obtained as the solution of the radial two-body Schrödinger equation with the corresponding potential. The normalization constants in the expression above are such that the plane wave expansion (40) is recovered in the free case, assuming the "free" normalization $u_{fi}/kr \xrightarrow{\text{free}} \delta_{fi} j_\ell(kr)$.

If the potentials we are dealing with are of short-range character, i.e., they vanish asymptotically faster than $1/r^2$, the asymptotic behaviour of the u_{fi}-functions will be given by a linear combination of the two independent free solutions, namely, the spherical Hankel functions of first and second kind: $h^{(1)}_\ell = j_\ell + i\eta_\ell$ and $h^{(2)}_\ell = j_\ell - i\eta_\ell$, where η_ℓ is the irregular spherical Bessel function. Therefore, the asymptotic general solution can be written as:

$$\frac{u_{fi}(r)}{kr} \overset{r\to\infty}{\longrightarrow} a h^{(2)}_\ell(kr) + b\mathcal{S}_{fi} h^{(1)}_\ell(kr), \tag{42}$$

where we have made explicit the dependence of u_{fi} on $\mathcal{S}_{fi}$ as a factor multiplying $h^{(1)}_\ell$. We could equally have chosen $\mathcal{S}_{fi}$ multiplying $h^{(2)}_\ell$ instead. The reason for this choice, which could look somewhat arbitrary, will be seen later on.

Since in the case of no interaction ($\mathcal{S}_{fi} = \delta_{fi}$) the plane wave (40) has to be recovered, we must have $a h^{(2)}_\ell(kr) + b\delta_{fi} h^{(1)}_\ell(kr) = \delta_{fi} j_\ell(kr)$, which necessarily implies $a = \delta_{fi}/2$ and $b = 1/2$, and therefore

$$\frac{u_{fi}(r)}{kr} \overset{r\to\infty}{\longrightarrow} \frac{1}{2}\left(\delta_{fi} h^{(2)}_\ell(kr) + \mathcal{S}_{fi} h^{(1)}_\ell(kr)\right). \tag{43}$$

If we now insert Eq.(43) into Eq.(41), and use the asymptotic form of $h^{(1)}_\ell$ [8], we then get:

$$\Psi_{\boldsymbol{k}}(\boldsymbol{r}) \overset{r\to\infty}{\longrightarrow} e^{i\boldsymbol{k}\cdot\boldsymbol{r}} + f(\Omega)\frac{e^{ikr}}{r} \tag{44}$$

where $f(\Omega)$ is the so-called *transition amplitude*.

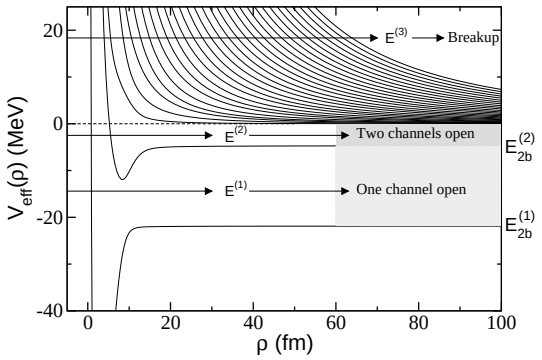

Fig. 3 Effective adiabatic potentials for a three-body system with two two-body bound states with energies $E_{2b}^{(1)}$ and $E_{2b}^{(2)}$. For a given three-body energy E, when $E_{2b}^{(1)} < E < E_{2b}^{(2)}$ only one channel is open; when $E_{2b}^{(2)} < E < 0$, both channels are open, and for $E > 0$ the breakup channel is also open.

Note that Eq.(44) represents and incoming plane wave, and an outgoing spherical scattering wave. This result justifies the in principle arbitrary choice made in Eq.(42). If we had taken $\mathcal{S}_{fi}$ multiplying $h_\ell^{(2)}$ instead, we would have got an incoming spherical wave after the collision, which is counter-intuitive after a scattering reaction. In any case, this is to some extent a non relevant issue, since one choice is just the complex conjugate of the other one.

Finally, the cross section for the reaction is given by the outgoing flux of particles through an element of surface normalized with the incident flux $d\sigma = j_{out} dS / j_{inc}$, where the flux of particles is defined as:

$$\boldsymbol{j} = \frac{\hbar}{2\mu i} \left[\Psi_{\boldsymbol{k}}^* \boldsymbol{\nabla} \Psi_{\boldsymbol{k}} - (\boldsymbol{\nabla} \Psi_{\boldsymbol{k}}^*) \Psi_{\boldsymbol{k}} \right]. \tag{45}$$

According to Eq.(44) the incoming wave is just $e^{i\boldsymbol{k}\cdot\boldsymbol{r}}$, from which one easily gets $j_{inc} = \hbar k/\mu$. The outgoing wave is $f(\Omega)e^{ikr}/r$, which after using Eq.(45) leads to $j_{out} = \hbar k |f(\Omega)|^2/\mu r^2$. Since the element of surface is $dS = r^2 d\Omega$ we finally obtain the well-known result $d\sigma/d\Omega = |f(\Omega)|^2$, which after integration over Ω leads to the final expression for the total cross section:

$$\sigma = \frac{\pi}{k^2} \sum_{i,f} |\mathcal{S}_{fi} - \delta_{fi}|^2. \tag{46}$$

In case of central potentials ℓ and m are good quantum numbers, and $u_{fi} = u_\ell \delta_{fi}$ and $\mathcal{S}_{fi} = \mathcal{S}_\ell \delta_{fi}$, and the expressions above lead to the well-known partial wave expansions of the transition amplitude and the elastic cross section. In this case the $\mathcal{S}$-matrix is therefore diagonal, and due to its unitary character each diagonal term can be written as $\mathcal{S}_\ell = e^{2i\delta_\ell}$, where δ_ℓ is the *phase shift*.

4.2 The three-body case with central potentials

At the three-body level the continuum wave functions appear as solutions of the coupled set of equations (16) when working in the hyperspherical expansion method, or equations (21) when working in the adiabatic expansion method. In (16) the potential matrix elements are not diagonal in the $\{\mathcal{Y}^{LM}_{K\ell_x\ell_y}\}$ basis, and in (21) the different adiabatic channels are mixed by means of the $P_{nn'}$ and $Q_{nn'}$ functions. In other words, a three-body scattering process is equivalent to a multichannel reaction, with, in general, a non-diagonal $\mathcal{S}$-matrix whose dimension is dictated by the number of channels open.

A very important advantage of the adiabatic expansion method is that the channels corresponding to a particle plus a bound dimer structure are associated to a single adiabatic channel. As an example, we show in Fig. 3 the typical behavior of the effective adiabatic potentials (Eq.(26)) for a three-body system where two of the two-body subsystems have a bound state. This is reflected in the fact that the two lowest effective adiabatic potentials go asymptotically to the binding energies $E_{2b}^{(1)}$ and $E_{2b}^{(2)}$ of each bound two-body system. In the figure, the different regions defined by the energy of the incident

particles are depicted. All the three-body energies E such that $E_{2b}^{(1)} < E < E_{2b}^{(2)}$ (such as $E^{(1)}$ in Fig. 3) correspond to processes where only one channel is open. Only the elastic collision between the third particle and the bound two-body state with energy $E_{2b}^{(1)}$ is possible. When the three-body energy increases up to the region $E_{2b}^{(2)} < E < 0$ ($E^{(2)}$ in the figure), a second channel is open. Two different collisions are now possible, the one where a particle hits the bound state with binding energy $E_{2b}^{(1)}$ and the one where a particle hits the state with binding energy $E_{2b}^{(2)}$. In the same way, each of these reactions has two possible outgoing channels, corresponding to the two allowed bound two-body states and the third particle in the continuum. In other words, in this energy range the inelastic (if the two bound two-body states correspond to the same subsystem) or transfer (if the two bound two-body states correspond to different subsystems) channel is open. When $E > 0$ (such as $E^{(3)}$ in Fig. 3), the breakup channel is also open, and it is described by the remaining infinitely many adiabatic potentials.

Summarizing, use of the adiabatic expansion method permits to easily identify 1+2 collisions, which can lead to the same or another 1+2 channel ($1+2 \to 1+2$ reactions, i.e., elastic or transfer processes) or to a pure continuum outgoing channel ($1 + 2 \to 3$ reactions, i.e., breakup reactions), and pure three-body collisions, which can lead to outgoing three-body continuum states ($3 \to 3$ reactions) or to a 1+2 channel ($3 \to 1 + 2$ reactions, i.e., recombination process). See [11] for details.

4.2.1 $3 \to 3$ *reactions*

Let us start with a three-body system such that none of the internal two-body subsystems is bound. In this case the only possible scattering reaction corresponds to a $3 \to 3$ process, which, although difficult to implement experimentally, can play a relevant role in nuclear astrophysics. The effective adiabatic potentials (26) behave asymptotically as $V_n^{eff} \propto (K + 3/2)(K + 5/2)/\rho^2$, which associates each adiabatic channel n to some particular value of the hypermomentum K. In this case the three body energy E is always positive (otherwise all the channels are closed), and in principle all the infinitely many adiabatic channels are open. Therefore, some truncation is necessary, and the size of the $\mathcal{S}$-matrix is determined by the number of terms included in the expansion (18). Usually the number of channels required to get convergence in the observables is clearly smaller than when using the hyperspherical harmonic expansion.

The generalization to the three-body case of the continuum wave function (41) is given by [12]:

$$\Psi_{\boldsymbol{k}_x\boldsymbol{k}_y}(\boldsymbol{x},\boldsymbol{y}) = (2\pi)^3 \sum_{LM}\sum_{nn'} \frac{i^K}{(\kappa\rho)^{5/2}} f_{nn'}(\rho)\Phi_n^{LM}(\rho,\Omega_\rho)\Phi_{n'}^{*LM}(\kappa,\Omega_\kappa), \tag{47}$$

where $\boldsymbol{k}_x$ and $\boldsymbol{k}_y$ are the linear momenta associated to the Jacobi coordinates $\boldsymbol{x}$ and $\boldsymbol{y}$, from which one can define $\kappa = \sqrt{k_x^2 + k_y^2}$ and the five hyperangles in momentum space $\Omega_\kappa \equiv \{\Omega_{k_x}, \Omega_{k_y}, \alpha_\kappa\}$, where $\tan\alpha_\kappa = k_x/k_y$. The angles Ω_ρ are the usual five hyperangles in coordinate space. In the expression above $\{\boldsymbol{k}_x, \boldsymbol{k}_y\} \equiv \{\kappa, \Omega_\kappa\}$ determines the energy $E = \hbar^2\kappa^2/2m$ and the directions of the momenta in the incident channel n', and n corresponds to the outgoing channel, where the particles move according to the directions given by Ω_ρ.

As previously discussed, in the case of no interaction, the angular eigenfunctions Φ_n reduce to the hyperspherical harmonics (assuming short-range potentials), and the matrix $(f_{nn'})$ of the radial wave functions is diagonal, where each diagonal term $f_{nn}(\rho)$ is nothing but the regular solution of Eq.(21) with $\lambda_n(\rho) = K(K + 4)$ and where the coupling terms $P_{nn'}$ and $Q_{nn'}$ are equal to zero.

In particular, if the regular solution is normalized such that $f_{nn}^{free}(\rho) = \sqrt{\kappa\rho}J_{K+2}(\kappa\rho)$, we then get that the expansion (47) becomes the usual partial wave expansion of the plane wave for three particles:

$$e^{i(\boldsymbol{k}_x\cdot\boldsymbol{x}+\boldsymbol{k}_y\cdot\boldsymbol{y})} = (2\pi)^3 \sum_{LM}\sum_{K\ell_x\ell_y} i^K \frac{J_{K+2}(\rho)}{(\kappa\rho)^2} \mathcal{Y}_{K\ell_x\ell_y}^{LM}(\rho,\Omega_\rho)\mathcal{Y}_{K\ell_x\ell_y}^{*LM}(\kappa,\Omega_\kappa). \tag{48}$$

Asymptotically, and assuming as usual short-range potentials, the coupled equations (21) do actually decouple, and, therefore, the asymptotic behaviour of the radial wave functions $f_{nn'}$ will be a linear combination of the two linearly independent free solutions, namely, $\sqrt{\kappa\rho}H_{K+2}^{(1)}(\kappa\rho)$ and $\sqrt{\kappa\rho}H_{K+2}^{(2)}(\kappa\rho)$:

$$f_{nn'}(\rho) \overset{\rho\to\infty}{\longrightarrow} \sqrt{\kappa\rho}(aH_{K+2}^{(2)} + b\mathcal{S}_{nn'}H_{K+2}^{(1)}), \tag{49}$$

which, as in the two-body case, must reduce to $\sqrt{\kappa\rho}J_{K+2}(\kappa\rho)$ in the free case ($\mathcal{S}_{nn'} = \delta_{nn'}$), leading to $a = \delta_{nn'}/2$ and $b = 1/2$. Therefore, the asymptotic behaviour of the radial wave functions $f_{nn'}$ contained in the expansion (47) is given by:

$$f_{nn'}(\rho) \overset{\rho\to\infty}{\longrightarrow} \frac{1}{2}\sqrt{\kappa\rho}\left(H^{(2)}_{K+2}\delta_{nn'} + \mathcal{S}_{nn'}H^{(1)}_{K+2}\right). \tag{50}$$

This expression can be written in a compact form as:

$$R \overset{\rho\to\infty}{\longrightarrow} \frac{1}{2}\sqrt{\kappa\rho}\left(H^{(2)} + \mathcal{S}H^{(1)}\right), \tag{51}$$

where $H^{(1)}$ and $H^{(2)}$ are diagonal matrices with diagonal terms $H^{(1,2)}_{K_i+2}$, where the index K_i is given by the asymptotic value $K_i(K_i+4)$ of the eigenfunction $\lambda_i(\rho)$ associated to the adiabatic channel i.

As done in the two-body case, after inserting Eq.(50) into (47) it is possible to write the asymptotic behaviour of the three-body wave function as

$$\Psi_{\boldsymbol{k}_x\boldsymbol{k}_y} \to e^{i(\boldsymbol{k}_x\cdot\boldsymbol{x}+\boldsymbol{k}_y\cdot\boldsymbol{y}_i)} + \mathcal{A}(\Omega_\rho)\frac{e^{i\kappa\rho}}{\rho^{5/2}}, \tag{52}$$

where

$$\mathcal{A}(\Omega_\rho) = (2\pi)^{5/2}\frac{e^{i\frac{3\pi}{4}}}{\kappa^{5/2}}\sum_{LM}\sum_{nn'}(\mathcal{S}_{nn'} - \delta_{nn'})\Phi^{LM}_n(\Omega_\rho)\Phi^{LM}_{n'}(\kappa,\Omega_\kappa), \tag{53}$$

is the $3 \to 3$ transition amplitude, where Ω_κ gives the directions of the incident momenta, and where we have taken into account that, asymptotically, the angular eigenfunctions Φ_n do not depend on the hyperradius.

The three-body incoming and outgoing flux is obtained similarly to the two-body case, after using analogous expressions for the current. This calculation involves several subtleties that are discussed in detail in [12]. In any case, the final result $d\sigma/d\Omega_\rho = |\mathcal{A}(\Omega_\rho)|^2$ is obtained, which is formally the same as found in two-body case. After integration over Ω_ρ and averaging over the incident Ω_κ angles ($\frac{1}{\pi^3}\int d\Omega_\kappa$) the following expression for the total cross section is obtained:

$$\sigma_{3\to3} = \frac{32\pi^2}{\kappa^5}\sum_L(2L+1)\sum_{nn'}\left|\mathcal{S}^L_{nn'} - \delta_{nn'}\right|^2 \tag{54}$$

which is equivalent to Eq.(46) for $3 \to 3$ reactions.

The expression above is in fact more general than for $3 \to 3$ reactions. It is also valid when the outgoing channel is a 1+2 channel ($3 \to 1+2$ reaction), i.e., a recombination process. In this case, since obviously $n \neq n'$ we have:

$$\sigma_{3\to1+2} = \frac{32\pi^2}{\kappa^5}\sum_L(2L+1)\sum_{n'\neq1+2}\left|\mathcal{S}^L_{nn'}\right|^2, \tag{55}$$

where n refers to the adiabatic channel associated to the dimer populated in the final state.

4.2.2 1+2 reactions

For this kind of reactions one could in principle make the same kind of analysis as in the previous subsection. However, it is simpler to realize that these reactions are actually two-body processes, which means that Eq.(46) does actually apply.

If we assume that the total three-body angular momentum L and projection M are good quantum numbers, we can then characterize the incoming and outgoing channels as $|i\rangle \equiv |n'L'M'\rangle$ and $|f\rangle \equiv |nLM\rangle$, respectively. If, furthermore, we assume that the two-body interactions are such that L and M are conserved, we then have that $\delta_{if} \equiv \delta_{nn'}\delta_{LL'}\delta_{MM'}$ and $\mathcal{S}_{if} \equiv \mathcal{S}_{nn'}\delta_{LL'}\delta_{MM'}$, which, after substitution in Eq.(46) permits to obtain:

$$\sigma = \frac{\pi}{p_y^2}\sum_{nn'}\sum_L(2L+1)|\mathcal{S}_{nn'} - \delta_{nn'}|^2, \tag{56}$$

where p_y is the particle-dimer relative momentum.

More specifically, if the outgoing channel is a pure three-body channel ($n \neq n'$) the expression above becomes

$$\sigma_{1+2\to 3} = \frac{\pi}{p_y^2}\sum_L (2L+1)\sum_{n\neq 1+2} |\mathcal{S}^L_{nn_i}|^2, \tag{57}$$

which gives the total breakup cross section for a process where the third particle hits the dimer associated to the adiabatic channel n_i with center of mass energy $E_{inc} = \hbar^2 p_y^2/(2\mu_{pd})$, where μ_{pd} is the particle-dimer reduced mass.

In the same way, when the outgoing channel is a 1+2 channel, the cross section (56) takes the form

$$\sigma_{1+2\to 1+2} = \frac{\pi}{p_y^2}\sum_L (2L+1)\sum_{n=1+2} |\mathcal{S}^L_{nn_i} - \delta_{nn_i}|^2, \tag{58}$$

which gives the cross section for a process where the third particle hits the dimer associated to the adiabatic channel n_i going out through another 1+2 channel. If we want to specify the outgoing 1+2 channel the summation over n in the expression above should be removed, and n would correspond to the specific chosen outgoing channel.

4.3 Calculation of the $\mathcal{S}$-matrix: Integral relations

Let us start by rewriting the general form of the continuum wave function (47) as:

$$\Psi_{\boldsymbol{k}_x\boldsymbol{k}_y}(\boldsymbol{x},\boldsymbol{y}) = (2\pi)^3 \sum_{LM}\sum_{n'=1}^{n_0} \frac{i^K}{\kappa^{5/2}} \Psi^{(n')}_{\boldsymbol{k}_x\boldsymbol{k}_y} \Phi^{*LM}_{n'}(\kappa,\Omega_\kappa), \tag{59}$$

where n_0 is the number of open channels and

$$\Psi_{n'} \equiv \Psi^{(n')}_{\boldsymbol{k}_x\boldsymbol{k}_y} = \frac{1}{\rho^{5/2}}\sum_{n=1}^{n_A} f_{nn'}(\rho)\Phi_n(\rho,\Omega_\rho). \tag{60}$$

This last expression is precisely the usual adiabatic expansion (18), and represents the three-body wave function for the incoming channel n'. The number n_A is the number of adiabatic channels used in the, in principle, infinite expansion. In general we have $n_A = n_0$, except for $1+2$ reactions below the breakup threshold. In this case n_0 is the number of 1+2 channels open, which is a finite and usually a very small number [12]. In a compact form the full wave function Ψ can be written as:

$$\Psi = \begin{pmatrix} \Psi_1 \\ \Psi_2 \\ \vdots \\ \Psi_{n_0} \end{pmatrix} = \frac{1}{\rho^{5/2}} \begin{pmatrix} f_{11} & f_{21} & \cdots & f_{n_A 1} \\ f_{12} & f_{22} & \cdots & f_{n_A 2} \\ \vdots & \vdots & \vdots & \vdots \\ f_{1n_0} & f_{2n_0} & \cdots & f_{n_A n_0} \end{pmatrix} \begin{pmatrix} \Phi_1 \\ \Phi_2 \\ \vdots \\ \Phi_{n_A} \end{pmatrix} = \frac{1}{\rho^{5/2}} R\Phi. \tag{61}$$

Since the asymptotic behaviour of the radial matrix R goes as given in Eq.(51) we then have:

$$\Psi \overset{\rho\to\infty}{\longrightarrow} \frac{1}{\rho^{5/2}}\frac{\sqrt{\kappa\rho}}{2}\left(H^{(2)} + \mathcal{S}H^{(1)}\right)\Phi = F + \mathcal{S}G, \tag{62}$$

where F and G are column vectors with n_0 terms whose i^{th} term is given by $\frac{\sqrt{\kappa\rho}}{2\rho^{5/2}} H^{(2)}_{K_i+2}\Phi_{n_i}(\rho,\Omega)$ and $\frac{\sqrt{\kappa\rho}}{2\rho^{5/2}} H^{(1)}_{K_i+2}\Phi_{n_i}(\rho,\Omega)$, respectively, with the understanding that in case that n_i is a 1+2 channel then the index of the Hankel functions has to be replaced by $\ell_y + 1/2$ and their argument by $k_y^{(n_i)} y$. Also, if we replace the Hankel functions in F and G by the regular and irregular Bessel functions, respectively, we get $\Psi \to F - \mathcal{K}G$, where $\mathcal{K}$ is the $\mathcal{K}$-matrix.

Once the numerical problem has been solved, and the radial wave functions for all the possible incoming channels have been obtained, we know that the full function Ψ behaves asymptotically as

$$\Psi \to AF + BG = A\left(F + \mathcal{S}G\right), \tag{63}$$

where A and B are $n_0 \times n_0$ matrices and where, obviously, $\mathcal{S} = A^{-1}B$.

Therefore, in principle, direct comparison of the numerically computed wave function with Eq.(63) would permit to extract the A and B matrices, and therefore $\mathcal{S}$. However, as shown in [13], when two-body dimers exist, the convergence of the adiabatic expansion is far too slow, and the fast convergence observed when describing bound states is lost.

In order to develop another method to extract the $\mathcal{S}$-matrix let us recall the second Green's identity:

$$\int_{\partial D} (\phi \boldsymbol{\nabla}\psi - \psi \boldsymbol{\nabla}\phi) \cdot \hat{n} dS = \int_D (\phi \nabla^2 \psi - \psi \nabla^2 \Phi) dV, \tag{64}$$

where ∂D is the boundary of the volume D, and $\hat{n}$ is the unitary vector normal to the surface ∂D.

Let us then consider a hypersphere V_ρ with radius ρ and its corresponding surface S_ρ. Following the equation above we can then write:

$$\int_{S_\rho} \left(\Psi \boldsymbol{\nabla} G^\dagger - (\boldsymbol{\nabla}\Psi) G^\dagger\right) \cdot \hat{n} dS = \int_{V_\rho} \left(\Psi \nabla^2 G^\dagger - (\nabla^2 \Psi) G^\dagger\right) dV, \tag{65}$$

where Ψ, F, and G are the column vectors described below Eq.(62), and therefore, their corresponding adjoint ($\dagger$) are row vectors.

If we now make $\rho \to \infty$, the Ψ wave function in the left hand side of Eq.(65) is evaluated at infinity, which means that it can be replaced by its asymptotic form in Eq.(63). To make things a bit simpler one can take F and G in terms of the regular and irregular Bessel functions, as described under Eq.(62), in such a way that functions to be integrated in Eq.(65) are all real. In this way the left-hand and right-hand sides of Eq.(65) can be written, respectively, as $A\left(\langle F|\nabla^2|G\rangle - \langle G|\nabla^2|F\rangle^T\right)$ and $\langle \Psi|\nabla^2|G\rangle - \langle G|\nabla^2|\Psi\rangle^T$, from which it is simple to find that

$$A = -\frac{2m}{\hbar^2}\left(\langle \Psi|\hat{\mathcal{H}} - E|G\rangle - \langle G|\hat{\mathcal{H}} - E|\Psi\rangle^T\right), \tag{66}$$

where $\hat{\mathcal{H}}$ is the Hamiltonian of the system and we have taken into account that $\hat{\mathcal{H}} = -\hbar^2\nabla^2/2m + V$ and the terms containing the potential cancel out. The expression above has been obtained with the understanding that F and G are normalized in such a way that:

$$-\frac{2m}{\hbar^2}\left(\langle F|\hat{\mathcal{H}} - E|G\rangle - \langle G|\hat{\mathcal{H}} - E|F\rangle^T\right) = \mathbb{1}. \tag{67}$$

In the same way, if we replace G by F in Eq.(65) we then get:

$$B = \frac{2m}{\hbar^2}\left(\langle \Psi|\hat{\mathcal{H}} - E|F\rangle - \langle F|\hat{\mathcal{H}} - E|\Psi\rangle^T\right). \tag{68}$$

Since the function Ψ is computed to be a solution of the hamiltonian, it satisfies $(\hat{\mathcal{H}} - E)\Psi = 0$, which leads to the final expressions:

$$A = -\frac{2m}{\hbar^2}\langle \Psi|\hat{\mathcal{H}} - E|G\rangle \ ; \qquad B = \frac{2m}{\hbar^2}\langle \Psi|\hat{\mathcal{H}} - E|F\rangle, \tag{69}$$

which gives the $n_0 \times n_0$ matrices A and B. These expressions are valid when F and G are given in terms of Hankel functions ($\mathcal{S} = A^{-1}B$) or in terms of the regular and irregular Bessel functions ($\mathcal{K} = -A^{-1}B$). More specifically, the matrix elements A_{ij} and B_{ij} are given by

$$A_{ij} = -\frac{2m}{\hbar^2}\langle \Psi_i|\hat{\mathcal{H}} - E|G_j\rangle; \qquad B_{ij} = \frac{2m}{\hbar^2}\langle \Psi_i|\hat{\mathcal{H}} - E|F_j\rangle, \tag{70}$$

respectively, where Ψ_i is given by Eq.(60), which is the three-body wave function for the incoming channel i, and F_j and G_j are the j^{th} term of the column vectors described under Eq.(62).

Eqs.(69) or (70) are the so-called *Integral Relations*. Note that F and G are the free solutions of the hamiltonian, which implies that the matrix elements in Eqs.(69) involve integrals of the two-body potentials only. Therefore, by means of the integral relations the matrices A and B are obtained from the inner part of the wave functions. This fact in itself is able to reduce to a large extent the required

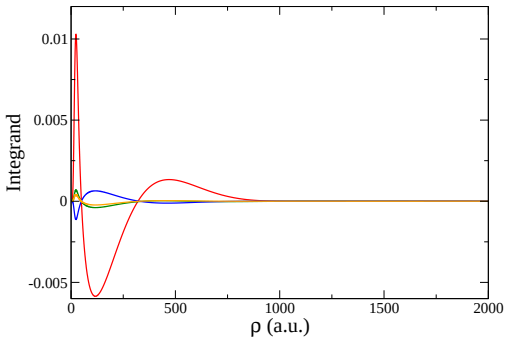

Fig. 4 Integrand contained in the integral relations for a system of three ^{4}He atoms. Calculations without use of the integral relations require knowledge of the wave functions up to more than 10^5 atomic units [14].

numerical effort. This is particularly true when the outgoing channel has 1+2 character. In this case, as we can see from Eq.(24), the corresponding angular eigenfunction (which actually enters in F and G) contains the dimer wave function, which contributes very significantly to reducing the size of the region relevant when applying the integral relations. This is illustrated in Fig.4, where a typical integrand involved in the integral relations is shown for the case of the Helium trimers [11]. Furthermore, the convergence of the $\mathcal{S}$-matrix in terms of the adiabatic channels included in the expansion (60) is now rather fast, often similar to the pattern of convergence observed when computing bound states.

A final remark is that the derivation shown here skips some of the deep details of the method. It can actually be proved that the integral relations are a consequence of the Kohn variational principle [15; 16], which establishes that if we consider a trial function Ψ_t for our three-body problem we then have that each matrix element $A^{-1}B + \frac{2m}{\hbar^2}A^{-1}\langle\Psi_t|\hat{\mathcal{H}} - E|\Psi_t\rangle\left(A^{-1}\right)^T$ is stationary with respect to variations in Ψ_t. From this principle it is possible to recover Eqs.(69) and at the same time prove that they are a second order correction of the matrices A and B.

4.4 Reactions in a stellar environment: Reaction rates

We have seen that for three colliding particles the cross section is given by Eqs.(54) and (55) for three-body and 1+2 outgoing channels, respectively. An important point not discussed so far, is that these cross sections are ill-defined, since they depend on the arbitrary normalization mass m through the three-body momentum $\kappa = \sqrt{2mE}/\hbar$. This is due to the fact that the incoming flux of particles is not well defined when two incident momenta are involved. In fact, as shown in [12], this flux is given by:

$$j_{inc} = \frac{\hbar\kappa}{m}\left(\frac{m}{\mu_x}\right)^{3/2}\left(\frac{m}{\mu_y}\right)^{3/2} = \sqrt{2E}\frac{m^{5/2}}{\mu_x^{3/2}\mu_y^{3/2}}. \tag{71}$$

However, for astrophysical reactions the relevant observable is not the cross section, but the reaction rate, which is defined as the cross section multiplied by the incoming flux of particles. Using then Eq.(71), (54), and (55) we easily get

$$R_{3\to3} = \frac{8\pi^2}{E^2}\frac{\hbar^5}{\mu_x^{3/2}\mu_y^{3/2}}\sum_L(2L+1)\sum_{nn'}\left|\mathcal{S}^L_{nn'} - \delta_{nn'}\right|^2, \tag{72}$$

$$R_{3\to1+2} = \frac{8\pi^2}{E^2}\frac{\hbar^5}{\mu_x^{3/2}\mu_y^{3/2}}\sum_L(2L+1)\sum_{n\neq1+2}\left|\mathcal{S}^L_{nn_i}\right|^2, \tag{73}$$

which are both independent of m and give, respectively, the reaction rates for a $3\to3$ process and a recombination process where the dimer associated to the channel n_i is formed.

When these reactions take place in a stellar environment, the energy of the particles is dictated by the temperature of the star. In a situation of thermal equilibrium, the probability for the particles

having an energy E for a temperature T is given by the Maxwell-Boltzmann distribution

$$B_N(E,T) = \frac{1}{\Gamma(\frac{3N-3}{2})}\frac{1}{K_BT}\left(\frac{E}{K_BT}\right)^{\frac{3N-5}{2}} e^{-\frac{E}{K_BT}}, \tag{74}$$

where N is the number of particles, K_B is the Boltzmann constant, and E is the center of mass energy.

It is then common, instead of the reaction rates themselves, to consider the energy-averaged reaction rate given by $\int dE B_N(E,T)R$, which for the particular case of three particles ($N=3$) is given by:

$$\langle R\rangle = \frac{1}{2}\frac{1}{(K_BT)^3}\int_0^\infty dE E^2 e^{-\frac{E}{K_BT}} R(E), \tag{75}$$

which is a function of the temperature, and where $R(E)$ is given by (72) or (73) for $3\to 3$ or $3\to 1+2$ reactions, respectively.

The same definition holds for a $1+2\to 3$ process. The incoming flux is the one of a two-body reaction ($\hbar p_y/\mu_{pd}$), and, by means of Eq.(74) for $N=2$, we then get the dissociation reaction rate:

$$\langle R_{1+2\to 3}\rangle = \sqrt{\frac{8}{\pi\mu_{pd}}}\frac{1}{(K_BT)^{3/2}}\int_0^\infty dE E e^{-\frac{E}{K_BT}}\sigma_{1+2\to 3}, \tag{76}$$

where here E is the relative projectile-dimer energy and μ_y the projectile-dimer reduced mass.

The exponential $e^{-\frac{E}{K_BT}}$ in the expression above makes the integrand negligible for energies just a few times bigger than K_BT. Since $K_B \approx 8.62\cdot 10^{-11}$ MeV/K, we have that for typical temperatures in the interior of a star ($\sim 10^7$ K), like the red giants where the helium burning takes place, the relevant energies are of the order the keV, which are very low at the nuclear scale, where typical separation or excitation energies are of the order of MeV.

Also, the cross sections, and therefore the reaction rates, are small at small energies and increase the value with E. The combination of this energy increasing function and the energy decreasing exponential in Eq.(75) or (76) determines the so-called *Gamow window*, which is the energy interval such that, for a given temperature, the reaction is more likely.

A second point to emphasize is that, as seen from Eqs.(55) and (57), the cross sections for the $3\to 1+2$ and the $1+2\to 3$ reactions are easily related by:

$$\sigma_{3\to 1+2} = 32\pi\frac{p_y^2}{\kappa^5}\sigma_{1+2\to 3}, \tag{77}$$

which is nothing but a consequence of the detailed balance principle, and permits to write

$$R_{3\to 1+2} = \frac{8\pi}{E^2}\frac{p_y^2\hbar^5}{\mu_x^{3/2}\mu_y^{3/2}}\sigma_{1+2\to 3}, \tag{78}$$

which together with Eqs.(75) and (76) leads to:

$$\langle R_{3\to 1+2}\rangle = \left(\frac{2\pi\hbar^2}{K_BT}\right)^{3/2}\left(\frac{\mu_{pd}}{\mu_x\mu_y}\right)^{3/2} e^{-\frac{B}{K_BT}}\langle R_{1+2\to 3}\rangle. \tag{79}$$

This expression relates the reaction rate for a three-body recombination process, for which experimental data are not possible, with the one of a breakup process, which is clearly more accessible from the experimental point of view.

So far we have implicitly assumed that all the particles involved in the reactions are not identical. In general, all the expressions for the cross sections and reactions rates should be multiplied by $\nu!$, where ν is the number of identical particles. Also, in the case of particles with non-zero spin, one has to include the degeneracy factors $g_i = 2j_i+1$, where j_i is the spin of particle i. When this is done we obtain the general form of Eq.(79):

$$\langle R_{3\to 1+2}\rangle = \nu!\frac{g_dg_p}{g_1g_2g_3}\left(\frac{2\pi\hbar^2}{K_BT}\right)^{3/2}\left(\frac{\mu_{pd}}{\mu_x\mu_y}\right)^{3/2} e^{-\frac{B}{K_BT}}\langle R_{1+2\to 3}\rangle, \tag{80}$$

which is Eq.(20) of the famous paper [17] about thermonuclear reaction rates.

From the results obtained for $R_{3\to 1+2}$ and $R_{1+2\to 3}$ it is easy to see that their corresponding dimensions are length to the sixth power divided by time, and length to the third power divided by time,respectively. These units look strange, and make apparently difficult to connect them with observables with physical meaning. However, let us remember that we are considering reactions taking place in a stellar environment. If we consider that in such an environment we have a particle density n_i for particle i (number of particles per unit volume), we can immediately see that the quantity $n_1 n_2 n_3 R_{3\to 1+2}$ is just the *production rate*, i.e., the number of reactions taking place per unit time and unit volume as a function of the temperature. The same happens for the breakup process after multiplying the reaction rate by the particle density of dimers and the density of particles hitting the dimer. It is common to give the number of particles per unit volume as $n_i = \rho N_A X_i / A_i$, where ρ is the mass density in the environment, X_i is mass ratio corresponding to particle i whose atomic mass is A_i, and N_A is the Avogadro number.

5 Resonant scattering

In order to clarify concepts, let us come back for a moment to the two-body case, where we saw that the asymptotic form of the wave function was given by Eq.(44), where the coefficient of the outgoing wave e^{ikr}/r (the scattering amplitude) measures the effect of the potential on the system.

Let us also recall that for bound states the asymptotic behaviour of the wave function is the exponentially decaying function $e^{-\kappa r}/r$, with $\kappa^2 = 2\mu|E_{2b}|/\hbar^2$, where E_{2b} is the binding energy and μ the reduced mass. We can immediately note that this asymptotic behavior can be obtained from the outgoing wave e^{ikr}/r simply by taking $k = i\kappa$. In general, the quantity of physical interest in Eq.(44) is the ratio of the coefficient of the outgoing wave to that of the incoming wave (this is actually what gives the $\mathcal{S}$-matrix, as seen for instance in Eq.(63)). Therefore, in the bound state case, where the outgoing wave (understood as a state with pure imaginary momentum) appears without an incident wave, we have that such a ratio is equal to infinity.

In other words, if we solve the two-body Schrödinger equation allowing complex momenta, we then have that bound states appear as poles of the $\mathcal{S}$-matrix in the positive imaginary axis of the complex momentum plane, whereas for real and positive values of k we have the region of physical scattering.

The fact that the $\mathcal{S}$-matrix must have a pole at $k = i\kappa$ and it must satisfy the unitarity condition for scattering states, suggests to write it in the vicinity of the pole as $\mathcal{S}(k) = (k + i\kappa)/(k - i\kappa)$. This form of the $\mathcal{S}$-matrix can be generalized to any pole, in particular for poles in the fourth quadrant of the momentum plane, i.e., poles at $k = k_r - ik_i$ $(k_r, k_i > 0)$. In this case we have:

$$\mathcal{S}(k) \approx \frac{k - (k_r + ik_i)}{k - (k_r - ik_i)} = \frac{(k - k_r) - ik_i}{(k - k_r) + ik_i}, \tag{81}$$

which is valid for k-values in the vicinity of the pole and maintains the unitarity condition.

Let us expand now the energy $E = \hbar^2 k^2/(2\mu)$ around $k = k_r$, which leads to $E - E_r \approx \hbar^2 k_r (k - k_r)/\mu$, where E_r is essentially the real part of $\hbar^2(k_r - ik_i)^2/(2\mu)$ (assuming $k_i \ll k_r$). Thus, after multiplying the numerator and denominator of Eq.(81) by $\hbar^2 k_r/\mu$ we get:

$$\mathcal{S} \approx \frac{(E - E_r) - i\Gamma_r/2}{(E - E_r) + i\Gamma_r/2} = 1 - \frac{i\Gamma_r}{(E - E_r) + i\Gamma_r/2} \tag{82}$$

where we have taken $\Gamma_r = 2\hbar^2 k_r k_i/\mu$, which is a positive quantity, since we have assumed the pole $k_r - ik_i$ to be in the fourth quadrant of the complex plane $(k_i > 0)$.

Therefore, if we consider a process like the one described in subsection 4.1, and make use of the form (46) for the total cross section, we get that if the pole appears for the partial wave ℓ, its contribution to the total cross section is given by:

$$\sigma_\ell = \frac{\pi}{k^2} \frac{(2\ell + 1)\Gamma_r^2}{(E - E_r)^2 + \Gamma_r^2/4}, \tag{83}$$

which is the *Breit-Wigner formula*, a Lorentzian peaked at $E = E_r$ with a width equal to Γ_r.

The physical meaning of these poles, whose complex energy is given by $E = E_r - i\Gamma_r/2 = \hbar^2(k_r - ik_i)^2/(2\mu)$, is what is known as a *Resonance* or *Quasi-bound* state. These states are associated to the existence of a potential barrier, in such a way that for energies below the height of the barrier the particles can be trapped by the potential for a finite lifetime, which is the time needed to quantum-tunneling the barrier, and then decay. The width of the resonance is related to the lifetime τ by means of the uncertainty principle relating the conjugate coordinates energy and time , i.e., $\Gamma_r = \hbar/\tau$. In this way we can see that the narrower the resonance the longer the lifetime. The fact that the particles are trapped in the resonant state for some time is the reason why the cross section, given by Eq.(83), presents a peak for collision energies close to the resonance energy.

By comparison of Eq.(46) for central potentials and (83) we can easily identify:

$$\sin^2\delta = \frac{\Gamma_r^2/4}{(E-E_r)^2 + \Gamma_r^2/4}, \tag{84}$$

from which it is simple to derive that $\tan\delta = \Gamma_r/2(E-E_r)$, which means that for $E = E_r$ the phase shift is equal to $\pi/2$. For this reason the energy of the resonance is often taken as the one at which the phase shift equals $\pi/2$. However, the equivalence between the resonance energy as a pole of the $\mathcal{S}$-matrix and as $\delta(E_r) = \pi/2$ is not exact. Only for very narrow resonances the two energies coincide.

Although the discussion in this section has been focused on two-body systems, the results are general. The main difference is that for more than two particles the problem is a multichannel problem, and therefore the $\mathcal{S}$-matrix becomes a true matrix. The expression (82) can be easily generalized, in such a way that the nn'-term of the $\mathcal{S}$ matrix can be written as:

$$\mathcal{S}_{nn'} \approx \delta_{nn'} - \frac{i(\Gamma_n\Gamma_{n'})^{1/2}}{(E-E_r) + i\Gamma/2}, \tag{85}$$

where Γ_n is the *partial width* for decay through channel n, and $\Gamma = \sum_n \Gamma_n$ is the total width.

From this expression we can for instance write the total cross section (54) for a system of three particles approaching to each other through channel n, and with a total energy close a resonance energy as:

$$\sigma_n^L = \frac{32\pi^2}{\kappa^5}(2L+1)\sum_{n'}\frac{\Gamma_n\Gamma_{n'}}{(E-E_r)^2 + \Gamma^2/4}, \tag{86}$$

which sums over all the possible outgoing channels n'.

Also, as we saw, for more than two particles the problem is a multichannel problem, and it is not so obvious how to determine the energy at which $\delta = \pi/2$. In this case it is more convenient to determine the complex energy at which the $\mathcal{S}$-matrix has a pole. An efficient procedure to do this will be described in the following subsection.

5.1 Resonances with the complex scaling method

As discussed above, a resonance is associated to a pole of the $\mathcal{S}$-matrix in the fourth quadrant of the energy plane. We have also learned that at the two- and three-body level the asymptotic form of the radial continuum wave functions is given by Eqs.(43) and (50), respectively, which means that at the resonance energy the coefficient multiplying $H^{(2)}$ is equal to zero, and the asymptotic form of the wave function is given by $H^{(1)}$ only. Since $H^{(1)}$ behaves at large distances as $H^{(1)} \to e^{i\kappa\rho}$, it is then trivial to see that when κ is located in the fourth quadrant of the complex plane ($\kappa = \kappa_r - i\kappa_i$) the resonance wave function diverges as $e^{\kappa_i\rho}$, with no contribution of the exponentially decaying term $H^{(2)}$. This balance between very large and very small numbers is rather delicate from the numerical point of view, and it makes the calculation of the precise energy of the resonance rather tricky.

A very efficient method that permits to overcome this problem is the *complex rotation* or *complex scaling* method. In this method all the radial coordinates are rotated into the complex plane by some arbitrary angle θ. This means that all the coordinates x_i given in Eq.(1) are transformed according to $x_i \to x_i e^{i\theta}$, whereas the polar and azimuthal angles Ω_{x_i} remain unchanged. According to this, from the definitions (3) it is simple to see that the hyper-radius is transformed in the same way ($\rho \to \rho e^{i\theta}$) and the hyperangles remain all unchanged. After this simple transformation is now easy to see that:

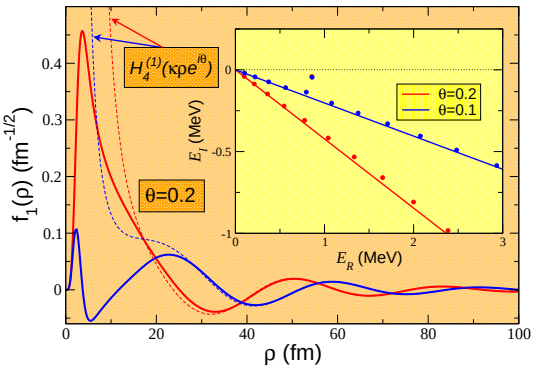

Fig. 5 Inner part: Complex rotated spectrum for the 2^+ states in ^{6}He for two different scaling angles. Outer part: Complex rotated radial wave function associated to the lowest adiabatic potential for the 2^+ resonance in ^{6}He. The thin dashed line is the Hankel function of first kind that gives the asymptotic behaviour.

1.- For a pole in the fourth quadrant of the complex plane the corresponding complex momentum is $\kappa = |\kappa|e^{-i\theta_r}$, with $0 < \theta_r \leq \pi/2$. Thus, after the transformation ($\rho \to \rho e^{i\theta}$) we have $i\kappa\rho \to i|\kappa|\rho e^{i(\theta-\theta_r)}$, or, in other words,

$$e^{i\kappa\rho} \to e^{i|\kappa|\rho\cos(\theta-\theta_r)}e^{-|\kappa|\rho\sin(\theta-\theta_r)}. \tag{87}$$

Therefore, after complex scaling, and provided $\theta > \theta_r$, the resonance wave function decays exponentially at large distances, exactly as a bound state. The resonances show up as "bound" states with complex energy $E = E_r - i\Gamma_r/2$, where Γ_r is the resonance width.

2.- For bound states, which appear as poles of the $\mathcal{S}$-matrix in the positive imaginary axis of the momentum plane, the same analysis as the one given above can be made ($\theta_r = -\pi/2$). It is then easy to find that after complex scaling the bound state wave function still goes exponentially to zero. The bound state spectrum is therefore still accessible after complex scaling.

3.- Ordinary continuum states do not correspond to poles of the $\mathcal{S}$-matrix, and therefore the asymptotic behaviour of the wave function (43) or (50) will contain both Hankel functions. Therefore, the asymptotic form will be a linear combination of an incoming wave $e^{-i\kappa\rho}$ and an outgoing wave $e^{i\kappa\rho}$. In principle, after the complex scaling transformation these two waves become $e^{-i\kappa\rho e^{i\theta}}$ and $e^{i\kappa\rho e^{i\theta}}$. However, in [18] it is proved that ordinary scattering wave functions do not depend on the scaling angle θ. The only possibility for that to happen is that, after the transformation, the momentum k associated to the continuum states transforms according to $k \to |k|e^{-i\theta}$. In other words, the energy of the continuum states transforms as $E \to Ee^{-i2\theta}$. Consequently, the complex-scaled scattering eigenfunctions have exactly the same asymptotical behavior as the unscaled states, but are associated, however, with a continuum which is rotated into the lower-half part of the complex energy plane by the angle 2θ.

All these features are illustrated in Fig. 5. The inner part shows the location in the fourth quadrant of the energy plane of the 2^+ states in the halo nucleus ^{6}He (^{4}He plus two neutrons) after a complex scaling transformation. Two different scaling angles, $\theta = 0.1$ rads and $\theta = 0.2$ rads, have been used. As we can see, the continuum states are rotated according to the θ-value. The isolated dot at about $E_R \approx 0.8$ MeV is θ-independent, and corresponds to the 2^+ resonance in ^{6}He, whose width is $\Gamma_R \approx 0.1$ MeV. The outer part gives the complex rotated radial wave function of the resonance associated to the lowest adiabatic potential. After the complex scaling transformation this radial wave function is complex, and the real and imaginary parts are given by the solid-red and solid-blue curves, respectively. The thin-dashed lines show the complex rotated Hankel function of first kind, which, as expected, matches with the computed wave function at large distances. The oscillating decaying asymptotic behaviour given in Eq.(87) can be clearly observed in the radial wave functions seen in the figure.

5.2 Radiative capture

It is important to note that the expressions given above for resonant scattering are still valid when dealing with radiative capture processes, like $a + b + c \to A + \gamma$, where A is a bound three-body state

having a, b, and c as constituents. If the initial three-body initial energy E is close to some resonance energy E_r, Eq.(86) still applies, and the cross section takes the form:

$$\sigma_{abc} = \frac{32\pi^2}{\kappa^5}\frac{2L+1}{g_a g_b g_c}\frac{\Gamma_{abc}\Gamma_\gamma}{(E-E_r)^2+\Gamma^2/4}, \tag{88}$$

where L is the resonance total angular momentum, Γ_{abc} is the width for the particle decay of the resonance into the resonance constituents, Γ_γ is the width for γ-decay of the resonance, and $\Gamma = \Gamma_{abc} + \Gamma_\gamma$ is the total width. In this expression we have included the degeneracy factors g_a, g_b, and g_c coming from the average of the initial states.

The inverse of the radiative capture process is the the photo-disintegration reaction $A+\gamma \to a+b+c$, whose cross section σ_γ is related to σ_{abc} through Eq.(77). Therefore:

$$\sigma_{abc} = \frac{32\pi}{\kappa^5}\frac{E_\gamma^2}{\hbar^2c^2}\frac{2g_A}{g_a g_b g_c}\sigma_\gamma, \tag{89}$$

where we have used that for a photon the incident momentum p_γ takes the form $p_\gamma = E_\gamma/\hbar c$, where E_γ is the photon energy. We have also taken into account that the degeneracy of the photon is equal to 2. From the expression above we then get the known result [19]:

$$\sigma_\gamma = \frac{2L+1}{2g_A}\frac{\pi\hbar^2c^2}{E_\gamma^2}\frac{\Gamma_{abc}\Gamma_\gamma}{(E-E_r)^2+\Gamma^2/4}. \tag{90}$$

As discussed in subsection 4.4, although the radiative capture cross section σ_{abc} is not well defined due to the dependence on the arbitrary normalization mass m, the radiative capture reaction rate is, and it is obtained after multiplication of σ_{abc} by the incoming flux of particles in Eq.(71):

$$R_{abc}(E) = \nu!\frac{\hbar^3}{c^2}\frac{8\pi}{(\mu_x\mu_y)^{3/2}}\frac{2g_A}{g_a g_b g_c}\left(\frac{E_\gamma}{E}\right)^2\sigma_\gamma(E_\gamma), \tag{91}$$

where we have introduced the number of identical particles ν, and where three-body energy E and the photon energy E_γ are related through the binding energy $B(<0)$ of the three-body system by $E = E_\gamma + B$.

As done in subsection 4.4, if we consider the particles in some environment in thermal equilibrium at some temperature T, we can average the reaction rate by means of the Maxwell-Boltzmann distribution (74). When done for $N = 3$ we obtain the general expression

$$\langle R_{abc}(E)\rangle = \nu!\frac{\hbar^3}{c^2}\frac{8\pi}{(\mu_x\mu_y)^{3/2}}\frac{g_A}{g_a g_b g_c}\frac{1}{(K_BT)^3}\int_0^\infty E_\gamma^2\sigma_\gamma(E_\gamma)e^{-\frac{E}{K_BT}}dE, \tag{92}$$

which is equivalent to Eq.(80) for a radiative capture process, and permits to obtain the reaction rate from the photo-disintegration cross section, for which experimental data are in principle more accessible. Therefore, in case of dealing with energies in the vicinity of a resonance, Eq.(90) permits an easy calculation of the reaction rate, provided Γ_{abc} and Γ_γ are known.

5.2.1 The sequential capture

Although not mentioned explicitly, in the discussion above it is assumed that the three particles a, b, and c, populate the three-body resonance in a direct way, i.e., without populating any intermediate two-body state. However, in case any of the two-body subsystems has a resonance at an energy smaller than E, it could happen that in a first step this two-body resonance is populated, and provided it lives long enough, then capture the third particle in a second step. This is a *sequential capture mechanism.*

It is quite clear that this mechanism amounts to two consecutive two-body processes. If the intermediate two-body state is formed by particles a and b the two-step process is then $a+b+c \to (ab)+c \to A+\gamma$. If the initial total energy is E, then, as before, we have $E = E_\gamma + B$. If we now call E' the relative energy between particle c and the ab system, and E'' the energy of the ab system, we then also have $E = E' + E''$.

As shown in [19; 20; 21], the reaction rate for to the sequential radiative capture process reads:

$$\langle R_{abc}(E',E'')\rangle = \frac{\nu!}{1+\delta_{ab}}\frac{g_A}{g_{ab}g_c}\frac{8\hbar}{\pi c^2}\frac{1}{\mu_{ab}^{1/2}\mu_{ab,c}^{3/2}}\frac{1}{(K_BT)^3}\int_0^\infty dE''E''\frac{\sigma_{ab}(E'')}{\Gamma_{ab}}\int_{E''}^\infty dEE_\gamma^2\sigma_\gamma(E_\gamma)e^{-\frac{E}{K_BT}}, \tag{93}$$

where

$$\sigma_{ab}(E'') = (1+\delta_{ab})\frac{g_{ab}}{g_ag_b}\frac{\pi}{k_{ab}^2}\frac{\Gamma_{ab}^2}{(E''-E_{ab})^2+\Gamma_{ab}^2/4}, \tag{94}$$

is the cross section for the formation of the two-body ab-resonance with energy E_{ab} and width Γ_{ab} ($\delta_{ab}=1$ if particles a and b are identical and zero otherwise), and the photo-dissociation cross section

$$\sigma_\gamma(E_\gamma) = \frac{2L+1}{2g_A}\frac{\pi\hbar^2c^2}{E_\gamma^2}\frac{\Gamma_{ab,c}\Gamma_\gamma}{(E-E_r)^2+\Gamma^2/4}, \tag{95}$$

is identical to Eq.(90) but where $\Gamma_{ab,c}$ is the width for decaying into the resonance ab plus particle c.

6 Concluding remarks

As mentioned in the introduction, one of the goals of these notes has been to describe the main aspects of the hyperspherical harmonic expansion and the adiabatic expansion methods, and show how these methods can be used to describe not only bound states but also scattering states. Together with this, we have also provided the expressions for the cross sections and reaction rates for three-body processes, paying particular attention to the calculation of the $\mathcal{S}$-matrix (integral relations) and resonances (complex scaling method).

Due to the space limitation, it has not been possible to include all along the way as many illustrations and examples as desired. However, they can easily be found in the literature. For instance, in [22] the hyperspherical harmonic expansion method is used to investigate ^{9}Be, and in [23] the α particle is investigated within the same model. Examples of use of the hyperspherical adiabatic expansion method are also numerous: The halo nuclei ^{11}Li and ^{6}He in [24; 25], ^{12}Be in [26], ^{17}Ne in [27]...

For the application of the integral relations to extract the $\mathcal{S}$-matrix and obtain the corresponding cross sections and reaction rates, the cases of $n-d$ scattering [11] or the Helium trimers [11; 28] are good examples. Also, in [16] the recombination process in the Li-He-He system was investigated.

Concerning resonances, examples of the use of the complex scaling method as a tool to extract energies and widths can be [29] for ^{5}H, [30; 31] for ^{9}Be, [32] for ^{11}Li, or [33] for ^{12}C. Note that the "bound state" asymptotic behaviour of the complex rotated resonance wave functions is maintained even when the Coulomb interaction is involved. Therefore the complex scaling method can be applied no matter the long- or short-range character of the interactions involved.

Finally, applications to nuclear astrophysics can be found in [34], where the different radiative capture processes involving neutrons and α-particles, leading to the production of ^{6}He, ^{9}Be, and ^{12}C, are analyzed. Particularly interesting is the competition between direct and sequential processes, which to a large extent determines the production rates at very low temperatures in systems like ^{9}Be [35] or ^{12}C (triple-alpha reaction) [19]. For these two last cases, where the Coulomb interaction enters, calculation of the continuum three-body wave functions is required. In order to overtake the problem of the unknown analytical form of the asymptotic continuum wave functions, these calculations are performed by discretizing the continuum spectrum by means of a box boundary condition, in such a way that the continuum states are treated as discrete states normalized to one inside the box.

References

1. M. Fabre de la Ripelle, The potential harmonic expansion method, Ann. Phys. **147**, 281 (1983)
2. M. Gattobigio, A. Kievsky, and M. Viviani, Nonsymmetrized hyperspherical harmonic basis for an A-body system. Phys. Rev. C **83**, 024001 (2011)
3. J. Raynal and J. Revai, Transformation coefficients in the hyperspherical approach to the three-body problem. Nuovo Cimento A **68**, 612 (1970)

4. M. Viviani, Transformation coefficients of hyperspherical harmonic functions of an A-body system. Few-Body Syst. **25**, 177 (1998)
5. E. Nielsen, D.V. Fedorov, A.S. Jensen, and E. Garrido, The three-body problem with short-range interactions. Phys. Rep. **347**, 373 (2001)
6. D.V. Fedorov and A.S. Jensen, Efimov effect in coordinate space Faddeev equations. Phys. Rev. Lett. **71**, 4103 (1993)
7. A.S. Jensen, E. Garrido, and D.V. Fedorov, Three-body systems with square-well potentials in $L = 0$ states. Few-Body Syst. **236**, 193 (1997)
8. M. Abramowitz and I.A. Stegun. *Handbook of mathematical functions.* Dover Publ., Inc. N.Y. (1965)
9. D.V. Fedorov and A. S. Jensen, Regularization of a three-body problem with zero-range potentials. J. Phys. A **3**, 6003 (2001)
10. M. Mikkelsen, A.S. Jensen, D.V. Fedorov, and N.T. Zinner, Three-body recombination of two-component cold atomic gases into deep dimers in an optical model. J. Phys. B **48**, 085301 (2015)
11. E. Garrido, C. Romero-Redondo, A. Kievsky, and M. Viviani, Integral relations and the adiabatic expansion method for 1+2 reactions above the breakup threshold: Helium trimers with soft-core potentials. Phys. Rev. A **86**, 052709 (2012)
12. E. Garrido, A. Kievsky, and M. Viviani, Breakup of three particles within the adiabatic expansion method. Phys. Rev. C **90**, 014607 (2014)
13. P. Barletta and A. Kievsky, Three-nucleon continuum by means of the hyperspherical adiabatic method. Few-Body Syst. **45**, 25 (2008)
14. H. Suno and B.D. Esry, Adiabatic hyperspherical study of triatomic helium systems. Phys. Rev. A **78**, 062701 (2008)
15. P. Barletta, C. Romero-Redondo, A. Kievsky, M. Viviani, and E. Garrido, Integral relations for three-body continuum states with the adiabatic expansion. Phys. Rev. Lett. **103**, 090402 (2009)
16. C. Romero-Redondo, E. Garrido, P. Barletta, A. Kievsky, and M. Viviani, General integral relations for the description of scattering states using the hyperspherical adiabatic basis. Phys. Rev. A **83**, 022705 (2011)
17. W.A. Fowler, G.R. Caughlan, and B.A. Zimmerman, Thermonuclear reaction rates. Annu. Rev. Astron. Astrophys. **5**, 525 (1967)
18. E. Balslev and J.M. Combes, Spectral properties of many-body Schrödinger operators with dilatation-analytic interactions. Comm. Math. Phys. **22**, 280 (1971)
19. E. Garrido, R. de Diego, D.V. Fedorov, and A.S. Jensen, Direct and sequential radiative three-body reaction rates at low temperatures. Eur. Phys. J. A **47**, 102 (2011)
20. K. Nomoto, F.K. Thielemann, and S. Miyajim The triple-alpha-reaction at low temperatures in accreting white dwarfs and neutron stars. Astron. Astrophys. **149**, 239 (1985)
21. C. Angulo et al., A compilation of charged-particle induced thermonuclear reaction rates, Nucl. Phys. A **656**, 3 (1999)
22. J. Casal, M. Rodríguez-Gallardo, J.M. Arias, and I.J. Thompson, Astrophysical reaction rate for ^{9}Be formation within a three-body approach. Phys. Rev. C **90**, 044304 (2014)
23. M. Viviani, A. Kievsky, and S.Y. Rosati, Calculation of the α-particle within the hyperspherical harmonic basis. Phys. Rev. C **71**, 024006 (2005)
24. E. Garrido, D.V. Fedorov, and A.S. Jensen, The ^{10}Li spectrum and the ^{11}Li properties. Nucl. Phys. A **700**, 117 (2002)
25. E. Garrido and E. Moya de Guerra, Electron scattering on two-neutron halo nuclei: The case of ^{6}He. Nucl. Phys. A **650**, 387 (1999)
26. C. Romero-Redondo, E. Garrido, D.V. Fedorov, and A.S. Jensen, Three-body structure of low-lying ^{12}Be states. Phys. Rev. C **77**, 054313 (2008)
27. E. Garrido, D.V. Fedorov, and A.S. Jensen, Three-body structure of the low-lying ^{17}Ne-states. Nucl. Phys. A **733**, 85 (2004)
28. A. Kievsky, E. Garrido, C. Romero-Redondo, and P. Barletta, The helium trimer with soft-core potentials. Few-Body Syst. **51**, 259 (2011)
29. R. de Diego, E. Garrido, D.V. Fedorov, and A.S. Jensen, Neutron-^{3}H potentials and the ^{5}H-properties. Nucl. Phys. A **786**, 71 (2007)
30. R. Álvarez Rodríguez, A.S. Jensen, E. Garrido, and D.V. Fedorov, Structure and three-body decay of ^{9}Be resonances. Phys. Rev. C **82**, 034001 (2010)
31. E. Garrido, D.V. Fedorov, and A.S. Jensen, Above threshold s-wave resonances illustrated by the states in ^{9}Be and ^{9}B. Phys. Lett. B **684**, 132 (2010)
32. E. Garrido, D.V. Fedorov, and A.S. Jensen, Dipole excited states in ^{11}Li with complex scaling. Nucl. Phys. A **708**, 277 (2002)
33. R. Álvarez Rodríguez, E. Garrido, A.S. Jensen, D.V. Fedorov, and H.O.U. Fynbo, Structure of low-lying ^{12}C resonances. Eur. Phys. J A **31**, 303 (2007)
34. R. de Diego, E. Garrido, D.V. Fedorov, and A.S. Jensen, Relative production rates of ^{6}He, ^{9}Be, ^{12}C in astrophysical environments. Europhys. Lett. **90**, 52001 (2010)
35. R. Álvarez Rodríguez, H.O.U. Fynbo, A.S. Jensen, and E. Garrido, Distinction between sequential and direct three-body decays. Phys. Rev. Lett. **100**, 192501 (2008)